Modelling & Implementation of a Heat Pump Coupled Between a Cooling Water Network and a Ventilation Unit

Anders Dorscheus Svoldgaard

Energy Technology, TEPE4-1005, 2021

Master's Thesis

STUDENT REPORT
AALBORG UNIVERSITY

Abstract

Denne kandidatafhandling omhandler implementering af et varmepumpe system koblet imellem et kølevandsnetværk på fabrikker og varme/kølebatterier i et ventilationssystem. Formålet er både at kunne reducere udledningen af CO2 samt at kunne reducere energiforbruget til opvarmning og køling på fabrikker. Baggrunden for projektet ligger i at Danfoss' CEO, Kim Fausing har udtalt at Danfoss skal være CO2-neutral i 2030. Mange af Danfoss' fabrikker rundt omkring i verden skal derfor renoveres for at kunne følge med i denne grønne omstilling. På de mange store fabrikker benyttes der den dag i dag et gasfyr eller rooftop chiller systemer, når der skal opvarmes eller køles. Problemet med disse systemer består i at de ofte er ineffektive og har en lav COP på omkring 2-3, og derudover udledes der CO2 i forbindelse afbrænding af naturgas i gasfyrene. På baggrund af dette skulle de gamle systemer kunne udskiftes med et varmepumpe system der er tilkoblet et ventilationsanlæg og kan derved udnytte spildvarmen fra produktionen der afsættes i kølevandsnettet. I forbindelse med dette projekt har der været et tæt samarbejde med Danfoss og NB-ventilation, som begge har kunne bidrage med data og praktisk erfaring forbindelse med udviklingen af dette system.

For at kunne beskrive og implementere dette system i praksis, var det nødvendigt at undersøge hvilke komponenter der var til rådighed på markedet og som levede op til kravene der var sat af Danfoss. Kravene til systemet var at det skulle håndtere luftmængder på 20,000 m^3/t hvoraf den maksimale køle- og varmekapacitet er henholdsvis 115 kW og 90 kW. Derudover skulle kompressoren også kunne styres med en frekvens regulator (VLT), der kan regulere køle- og varmeeffekten. I forbindelse med valget af kompressorer blev der dog ikke fundet en som både havde en VLT og kunne levere den ønskede effekt. Resultat blev at Danfoss kompressoren SY380-4 blev valgt, da den kunne levere den ønskede effekt, dog med det kompromis at den ikke kunne reguleres i praktisk. Kondensatoren og fordamperen der kunne benyttes, var fundet igennem i software fra Danfoss, hvorfra H118-E varmevekslerserien blev valgt. Da komponenterne var fundet, skulle der opstilles en model som kunne beskrive det samlede systems ydeevne. For at kunne modellere kompressoren, blev databladet anvendt hvorfra der blev opstillet tabeller. Igennem interpolation af tabellerende kunne kompressorens arbejde og massestrøm beskrives som funktion af fordampnings- og kondenseringstemperaturen. For at opstille en model af kondensatoren og fardamperen blev der ligeledes lavet tabeller baseret på Danfoss softwaren Hexact. Disse tabeller kunne ud fra massestrømmen af kølemiddel samt kondenserings- og fordampningstemperaturen beskrive varmeoverførslen i vekslerne. For at kunne kompensere for den manglende styring af kompressoren, blev kondenserings- og fordampningstemperaturen baseret på udløbs temperaturerne i fordamperen og kondensatoren. Da tilløbs temperaturerne var baseret på en simpel model af et køletårn varierede disse som funktion af udeluftens temperatur.

For at kunne beskrive systemets ydeevne baseret virkelige vejrforhold, blev vejrdata fra Frankfurt benyttet. Hertil blev "The Bin Method" anvendt til at opdele vejrdata i intervaller for forskellige temperaure og antal timer. Baseret på dette, kunne systemets varme- og køleevne beskrives over et helt år, antaget at det er placeret i Frankfurt. Ud fra modellen viste det sig at systemet kunne levere en COP på omkring 6.7 når der skulle varmes, og en COP på omkring 5.4 når der skulle køles. Modellen viste også at tillufts temperaturen til fabrikken var omkring 30 °C til 35 °C når der skulle varmes og omkring 21 °C når der skulle køles. Da den ønskede fabrikstemperatur er 22 °C til 23 °C kunne det konkluderes at den valgte kompressor er for stor til at opvarme med.

Slutteligt blev der også lavet en økonomiskanalyse af systemet, hvor tilbagebetalingsperioden samt drift- og investeringsomkostningerne blev beregnet. Disse var baseret på rigtige priser fra NB-ventilation og Danfoss, og giver derfor et godt estimat. Udover dette blev den samlede nutidsværdi af systemet, baseret på en 10 års periode for forskellige scenarier beregnet. Analysen viste at tilbagebetalingsperioden ligger på omkring 4 til 5 år sammenlignet med rooftop chillere, og har en investeringsomkostning på 675,893 kr. Det blev beregnet, at de årlige driftsomkostningerne for systemet er 265,348 kr. antaget en strømpris på 2 kr/kWh. Den samlede nutidsværd af systemet over 10 år blev beregnet til at ligge mellem 354,000 og 642,507 kr. afhængigt af system effektiviteten.

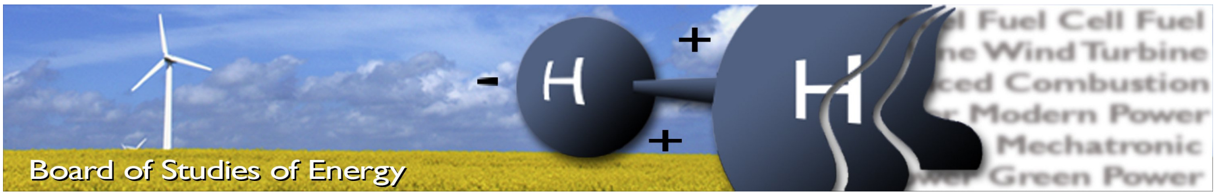

AALBORG UNIVERSITY
STUDENT REPORT

Title:
Modelling & Implementation of a Heat Pump Coupled Between a Cooling Water Network and a Ventilation Unit.

Theme:
Master's Thesis

Project period:
10^{th} Semester Spring 2021

ECTS:
30

Project group:
TEPE4-1005

Participants:

Anders Dorscheus Svoldgaard

Supervisors:
Mads Pagh Nielsen
Rasmus Hasselgren Gerhardt

Number of pages:
69

Submission date:
28-05-2021

Synopsis:

In this study, a heat pump system coupled between a cooling water network and a 20,000 m^3/h ventilation unit was analyzed and modelled. The system should replace low COP rooftop chiller systems and gas furnaces used for heating and cooling in factories. The objective was to determine the systems heating and cooling performance over a year based on weather data. The economical aspects in terms of the CAPEX, OPEX and repayment period was also examined in this study. Based on the model it was found that the system could achieve a COP of 5.4 for cooling and a COP of 6.7 for heating. The CAPEX for the system was found to be 675,893 DKK and the yearly OPEX was found to be 265,348 DKK. Based on this the repayment period was 4-5 years depending on the system performance.

Writers confirms in solidarity, that no plagiarism has occurred in this report.

Preface

This master's thesis was written by Anders D. Svoldgaard during the 4$^{\text{th}}$ semester of the Master's programme in Energy Engineering with specialization in Thermal Energy and Process Engineering at Aalborg University. The thesis is based upon a project proposal by Danfoss, as a part of making their factories world wide carbon neutral and improving their energy efficiency. The project concerns the implementation of a heat pump system coupled between the cooing water network in factories and the heating/cooling coils within a ventilation unit. The objective is to determine the system performance through a model and analyze the economical aspects such as the operational and capital expenditures. I would like to thank both *Per Højbjerre* and *Rasmus Hasselgren Gerhardt* from NB-ventilation, for providing both guidance and knowledge during this master's thesis. Furthermore, I would like to thank *Folke Hougaard Pedersen* from Danfoss for providing data used in this study and his expertise in terms of designing and implementing energy efficient system.

The following software programs were used during this project:

- **CoolSelector** - Used to acquire compressor data.
- **Engineering Equation Solver** - Used for modelling.
- **Hexact** - Used to acquire heat exchanger data.
- **Matlab** - Used for data processing and making plots.
- **Overleaf** - Used to write this project.

Reading Guide

References throughout this study are based upon the Vancouver method, from which a reference will be denoted by a number in the text. The number refers to the source which can be found in the bibliography and is described in the following order.

Author ∼ *Title* ∼ `URL` ∼ Year ∼ Notes

References which are denoted before a period in a sentence indicates that the sentence is referred to. References which are denoted after a period indicates that the section is referred to. Pictures, component prices and data without a source is either from NB-ventilation, TT-Coil or Danfoss which has allowed it to be used for this study. Generally, it will be mentioned in the text for example "The data provided by Danfoss" or "According to NB-ventilation". When an abbreviation is presented for the first time, the full word is denoted in brackets afterwards. An overview of the abbreviations used throughout this study can be found in the nomenclature along with symbols, superscripts and subscripts. The pages before the introduction are labeled with Roman numeral, afterwards they are labeled with numbers. Chapters throughout this study are labeled chronologically along with figures, tables, sections and equations for a given chapter. The appendices are labeled by letters in an alphabetically order. As an example, the first figure in chapter 6 will be labeled fig. 6.1 and the first figure in appendix B will be labeled B.1. Finally an overview of the chapters and section throughout this study can be seen in the table of contents.

Nomenclature

G	Mass velocity	$[kg/(m^2 \cdot s)]$
h_{fg}	Enthalpy of vaporization	$[kJ/kg]$
h	Enthalpy	$[kJ/kg]$
$\dot{m}$	Mass flow rate	$[kg/s]$
n	Amount of/number of	$[-]$
P	Power (Compressor/Cooling Tower)	$[kW]$
$\dot{Q}$	Heat transfer rate	$[kW]$
q''	Surface Heat Flux	$[kW]$
r	Inflation rate	$[-]$
T	Temperature	$[K]$, $[°C]$
V	Volume	$[m^3]$
$\dot{V}$	Volume flow	$[m^3/s]$
x	Quality	$[-]$

Greek Letter	**Description**	**Unit**
η	Efficiency	$[-]$
ρ	Density	$[kg/m^3]$
ω	Humidity ratio	$[-]$

Abbreviation	**Description**
AHU	Air Handling Unit
ASHRAE	American Society of Heating, Refrigerating and Air-conditioning Engineers
CAPEX	Capital Expenditures
CFC	Chlorofluorocarbon
CM	Contribution Margin
COP	Coefficient of Performance
DKK	Danish Krone
DP	Differential Pressure
EES	Engineering Equation Solver
EG	Ethylene Glycol
EU	European Union
GWP	Global Warming Potential
HFC	Hydrofluorocarbon
HFO	Hydrofluoroolefins
NPV	Net Present Value
ODP	Ozone Depletion Potential
OPEX	Operational Expenditures
ppm	Parts per Million
PV	Present Value
RPM	Rounds per minute
U.S.	The United States
VLT	Velocity Controller

Subscript	**Description**
1	Point 1 supply in AHU
2	Point 2 after heat exchanger in AHU
3	Point 3 exhaust in AHU
amb	Ambient
comp	Compressor
cond	Condenser
CT	Cooling Tower
CW	Cooling Water
EG	Brine (EG/water)
evap	Evaporator
he	Heat Exchanger
HP	Heat Pump
in	Inlet
lat	Latent
out	Outlet
R	Refrigeration
ref	Refrigerant
sensi	sensible
swept	Swept volume
v	Vapor
vol	Volumetric
wat	Water
WO	Cooling tower outlet water

Table of Contents

Chapter 1 Introduction **1**

Chapter 2 Problem Analysis **3**

2.1 System Overview 3

2.2 The Air Handling Unit 5

2.3 The Heat Pump System 7

2.4 Weather Data Analysis and Operating Hours 18

2.5 Problem Statement 20

Chapter 3 System Modelling **21**

3.1 Modelling of the Compressor 21

3.2 Modelling of the Condenser and Evaporator 22

3.3 Modelling of the Heating and Cooling Coils 25

3.4 Modelling of the AHU Heat Exchanger 29

3.5 Modelling of the Cooling Tower 30

Chapter 4 Modelling Results **31**

4.1 The Bin Data Method 31

4.2 System Performance During Heating Mode 33

4.3 System Performance During Cooling Mode 36

Chapter 5 Economical Analysis of the Heat Pump System **39**

5.1 System Design Considerations 39

5.2 Capital Expenditures 41

5.3 Operating Expenditures 42

5.4 Repayment Period 45

Chapter 6 Discussion **51**

6.1 System Designs and Components 51

6.2 Model Assumptions and Consideration 52

6.3 Future Choice of Refrigerant 53

6.4 Economical Aspects 54

6.5 Results 55

Chapter 7 Conclusion and Future Work **57**

Bibliography **59**

Appendix A Compressor Data sheets **63**

Appendix B Heating and Cooling Coil Specifications **67**

Appendix C Cooling Tower Performance **69**

Introduction

1

In the last century, the carbon emissions has greatly increased which is a result of industrial processes and the combustion of fossil fuels for energy production. This has resulted in an increased focus on reducing the global carbon emissions. In 2018, 80% of the U.S. energy production came from fossil fuels and 93% of the total carbon emissions was related to human activity. The emissions has an impact on the environment in terms of increased global surface temperatures and increasing water levels. As seen in fig. 1.1 both the global atmospheric concentration of CO_2 in parts per million (ppm) and the CO_2 -emissions has greatly increased since the mid 1800's. If the global energy consumption continues to rise and is based on fossil fuels, the concentration of carbon is estimated to reach 900 ppm by the end of the century. [1] [2]

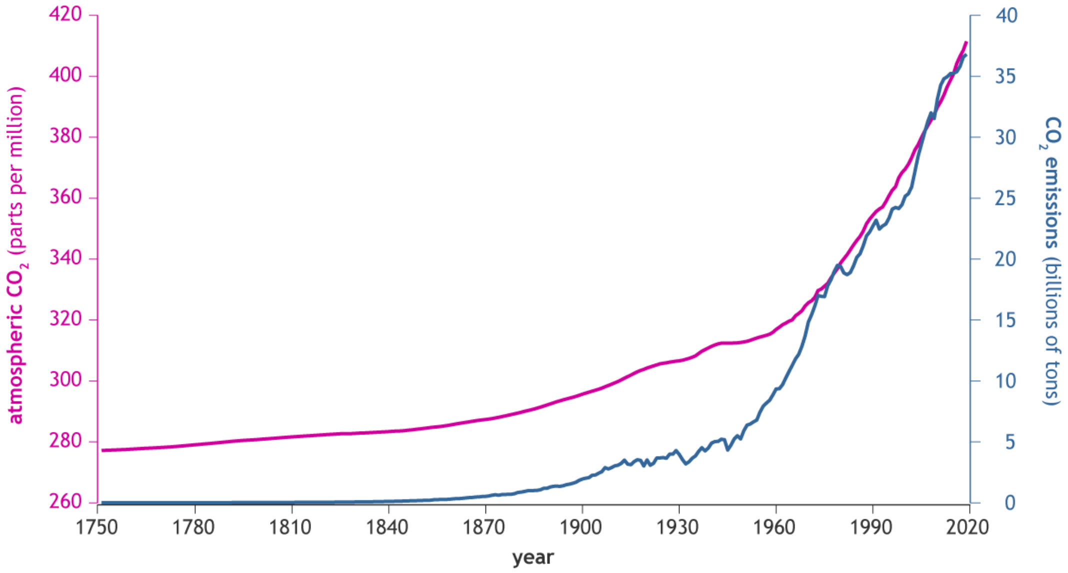

Figure 1.1. Measured atmospheric CO_2 concentration and CO_2 emissions from 1750 to 2020. [2]

The European Union (EU) has made climate strategies for 2030 and 2050. The strategies for 2030 includes goals such as a 40% reduction in carbon emissions compared to the 1990 level. Furthermore the strategy includes a goal of improving the general energy efficiency by 32%. According to the EU, the general energy efficiency can be improved through the implementation of more efficient heating and cooling systems along with energy renovations of elder buildings. The long term goal is to achieve a decarbonised and highly energy efficient building stock by 2050. [3] [4]

In the future more regulations and increased carbon taxes could affect companies and thereby force them to invest towards a green transition. Furthermore this could potentially save the companies money through energy optimization and also reduce their carbon emissions. Danfoss which is a major company with factories world wide has a set a target of becoming carbon-neutral by 2030. The CEO of Danfoss Kim Fausing, said that the target can be reached by utilizing surplus heat from production in factories. [5]

As a part of this Danfoss and NB-ventilation which is located in the northern Denmark and produces custom made ventilation systems for industrial applications mainly, has entered into a collaboration. The focus is to better utilize the energy from production in factories through air handling units (AHU's). The collaboration aims to utilize the excess energy from cooling water in combination with a heat pump to provide additional cooling and heating in ventilation systems. A common issue is that the machines within a factory are often air-cooled which increases inside air temperature and thus requires additional air conditioning. Therefore it is necessary that the heat produced by machines is removed through a cooling water system. The cooling water system is connected to a cooling tower from which heat can be released to the ambient air. By utilizing the heat pump the excess heat from production can be transferred around the factories and thus reduce the power consumption. [6]

The heat pump will be combined with a ventilation system from which it can cool and heat the supply air entering buildings. In the winter season when the heat recovery of a ventilation system is not sufficient to heat up the supply air, the heat pump system will activate and provide additional heating. In the summer season with high ambient air temperatures, the supply air can not be cooled sufficiently through a heat exchanger utilizing the exhaust air from the building. The heat pump system will therefore activate in a reversed cycle from which cooling of the supply air is provided. Due to condensation of the water content in the air when cooling, the required effect for cooling is greater than when heating. A future goal is to implement the system in the U.S. where factories typically uses natural gas for heating in the winter. Due to the low natural gas prices of approximately 5-7 øre/kWh it can be difficult for the heat pump system to become feasible. However Danfoss sees the combination of utilizing heat pumps along with energy optimization as the best solution for reducing expenses for heating and cooling while transitioning in to a carbon-neutral future. [6]

The plan is to build a $20.000\,\mathrm{m^3/h}$ prototype of the system by 2021 located at Danfoss Neumünster in Germany. The system will actually have a air capacity of $40.000\,\mathrm{m^3/h}$ due to dampers which can open in the summer season to provide additional free cooling. In order to build the prototype, NB-ventilation and Danfoss would like to acquire more knowledge about the system in terms of the required components for the heat pump system along with the performance and the cost of implementing the system.

Problem Analysis 2

The system to be implemented will indirectly connect the cooling water network in a factory to an AHU through a vapor compression cycle. In order to provide an overview of the system, a detailed explanation of the individual components and the processes will be presented in this chapter. Furthermore an analysis of the system configuration and the future choice of refrigerant be reviewed.

2.1 System Overview

The overall system to be build and implemented in Neumünster can be divided in to three elements, an AHU, a vapor compression cycle and a cooling tower. In the AHU there are heating and cooling coils which are connected to the vapor compression cycle through an evaporator. In the other part of the system the cooling water is connected to the condenser. Throughout this study, the system will be referred to as in 'Heating Mode' when the coils heats the air and 'Cooling Mode' when the coils cools down the air. An overview of the system in cooling mode can be seen in fig. 2.1.

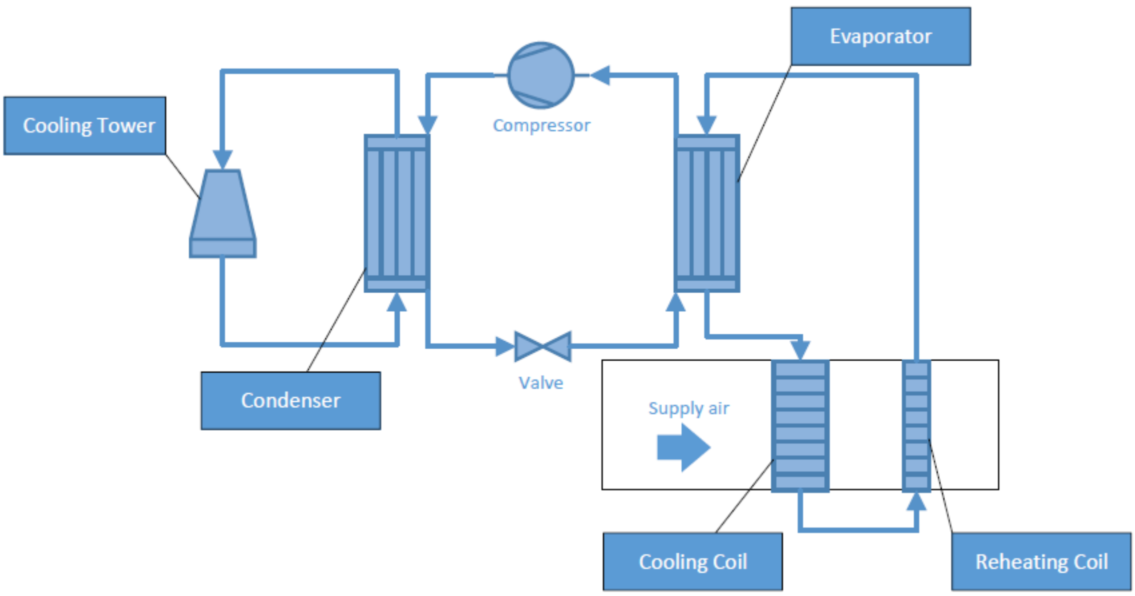

Figure 2.1. Overview of the heat pump system in operating in cooling mode.

It can be seen in fig. 2.1 on the preceding page that while the system operates in cooling mode the reheating and cooling coils are connected to an evaporator. Within the coils are a brine mixture of ethylene glycol (EG) and water in order to prevent freezing. As the mixture flows through the coils, heat is absorbed from the air.

A worst case scenario for operating during 'Cooling Mode' will be a combination of high ambient temperatures along with a high humidity. The air temperature during a worst case scenario will be around 27 °C when entering the cooling coil. The cooling coil cools the air down to 15 °C from which the moist content of the air condenses. After the cooling coil, the air flows through a reheating coil where the excess energy absorbed from the EG-water mixture reheats the supply air to 18 °C. The energy absorbed by the EG-mixture is then removed in the evaporator from which it is emitted to the cooling water through the condenser.

An illustration of the overall system operating in 'Heating Mode' can be seen in fig. 2.2. The system is generally identical, however the vapor compression cycle is now operating in a reversed configuration. When operating in 'Cooling Mode' the evaporator and condenser are counter-current heat exchangers, but as a result of operating in the reversed configuration the evaporator and condenser will become co-current heat exchanger. During operation in 'Heating Mode' the evaporator is absorbing energy from the cooling water which is emitted in the condenser such that the EG-water mixture is heated.

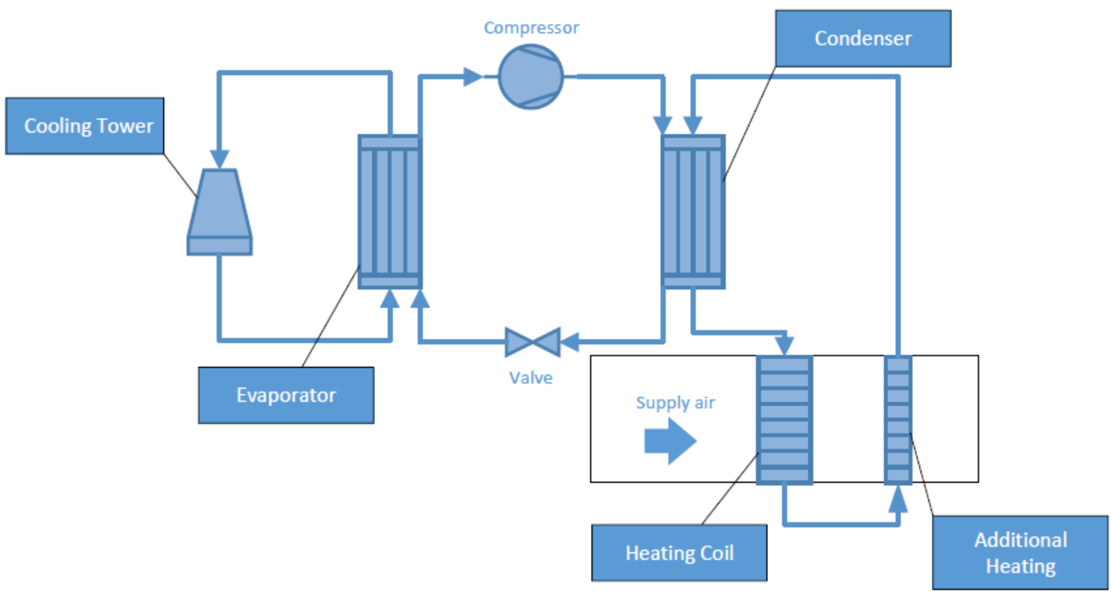

Figure 2.2. Overview of the heat pump system in heating mode.

In a worst case scenario during 'Heating Mode' the supply air enters the heating coil with a temperature of 17 °C. Both of the coils now operates as a single unit and heats the air to 30 °C. The required heating effect is lower than the cooling effect since no condensation of the air occurs. The cooling water temperature will also vary depending on the season since it utilizes ambient air to deposit energy.

2.2 The Air Handling Unit

The system will be based on the implementation of an AHU as described in chap. 1 on page 1. The primary functions of the AHU is to provide fresh air with low a CO_2 content to a building in order to provide a good indoor environment. In addition, some buildings also have certain requirements for the humidity and temperature of supply air. The AHU can therefore condition the supply air through components such as a heat exchanger for heat recovery and coils which can be used for heating, cooling and dehumidifying. The AHU also consists of minor components such as filters, dampers and ventilators which are used for filtering the outdoor air and controlling the air flow. NB-ventilation produces AHU's as seen in fig. 2.3, the AHU shown contains a double crossflow heat exchanger and still misses the exterior.

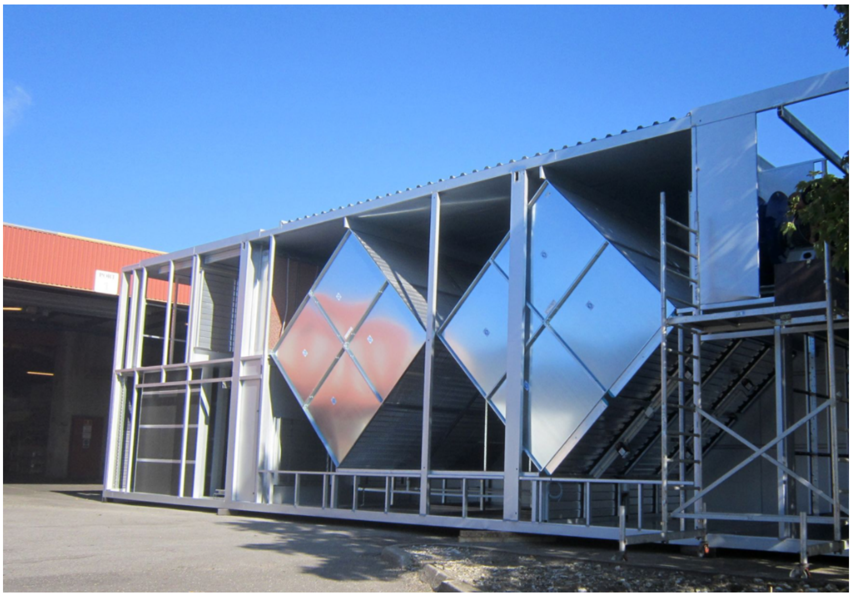

Figure 2.3. Illustration an AHU been produced at NB-ventilation.

There are multiple heat exchanger types which can be used in AHU's such as a crossflow, counterflow, double crossflow and an enthalpy wheel. The different types all have their advantages and disadvantages. The double crossflow heat exchanger has a efficiency of around 78-85 %. However the double crossflow heat exchanger takes up a lot of space and can therefore not be used for all applications. The reason why it is desired to use in combination with the heat pump system is that it consumes no energy while recovering energy from the exhaust air flow. An alternative heat exchanger to use for applications with limited space could be an enthalpy wheel. It works by rotating a wheel made of corrugated metal between the supply and exhaust air. The metal is heated directly by the exhaust air and then rotated to the supply air, which will be heated up as it flows through the wheel. An enthalpy wheel will not take up a lot of space and has a high efficiency of 75-88 %. The disadvantage is that it consumes energy through the motor used to rotate the wheel and it can break down during operation. Therefore, a double crossflow heat exchanger will be chosen for the prototype to been implemented in Neumünster.

The air flow through an AHU with a double crossflow heat exchanger can be seen in fig. 2.4. Here it can be seen that heat is recovered through the double crossflow heat exchanger and afterwards it is either heated or cooled by a coils. The heating and cooling coils contains a mixture of EG around 30 % and water. The reason for using the mixture is to prevent freezing of the water, which would otherwise result in an expansion of the water and therefore break the tubes within the coils.

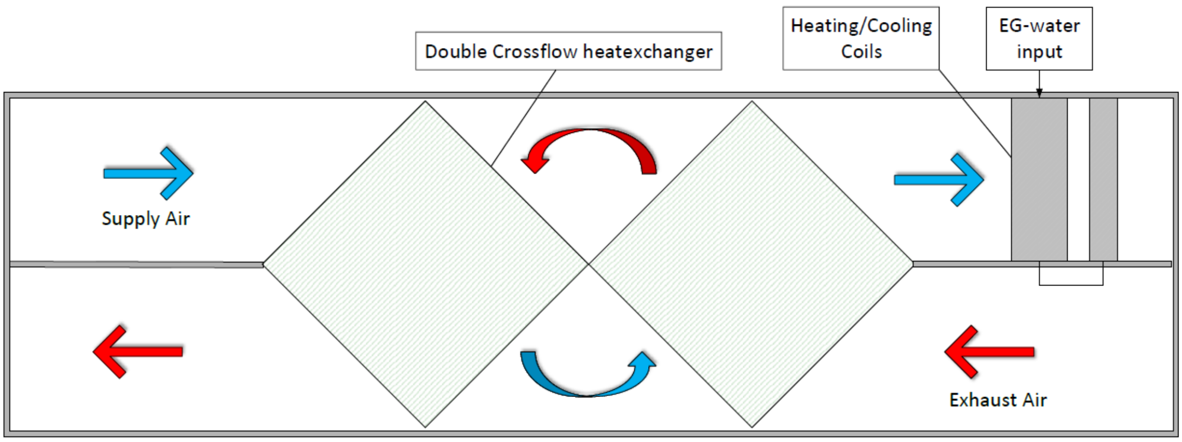

Figure 2.4. Illustration of the flow throughout an AHU.

The heating and cooling coils can also be connected to a recirculating system as an alternative. The purpose of a recirculation system is to recirculate the indoor air during periods where buildings are not occupied. By doing this, the factory facility can be maintained at a desired temperature while consuming a small amount of energy. The reason is that it will not be necessary to remove CO_2 content by adding fresh supply air which would require energy to be heated or cooled. The heating and cooling coils will be placed in an air duct as can be seen in fig. 2.5.

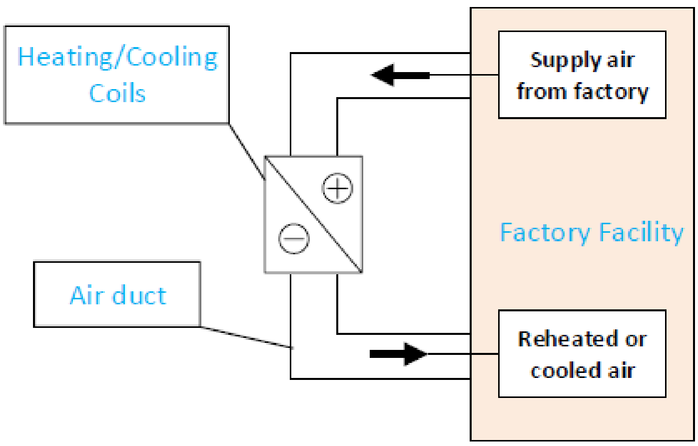

Figure 2.5. Illustration of an air recirculation system of the air.

The coils are connected to the vapor compression cycle, which will be utilizing the cooling water in the factory. When the building is about to be occupied again the AHU's will start up again and start to remove the CO_2 content in the air.

2.3 The Heat Pump System

The vapor compression cycle used for the system consists of two heat exchangers, an evaporator and a condenser along with a compressor and a valve. During this project it will be preferred to utilize components produced by Danfoss since these can be acquired at a reduced price and therefore reduce the expenses of this project. For the prototype system, Danfoss has suggested a compressor which can operate at a variable speed through a frequency controller (VLT) which can be adjusted between 30 Hz to 90 Hz. By utilizing the frequency controller the compressor can increase the refrigerant flow rate doing periods with high cooling or heating load. This ensures that the compressor power always matches the cooling or heat demand from which the energy consumption can be reduced. The compressor uses an old refrigerant type R407C which is being phased out in the near future. However the purpose is build and test the system from which the components will be replaced by newer technologies in the future. The choice of the future refrigerant is important since leakages of a system can contribute to global warming and depletion of the ozone layer, however it also affects the performance of vapor compression cycle.

The Choice of Refrigerant and Consideration

The reason why refrigerants are being phased out, is due to their GWP (Global Warming Potential) and their ODP (Ozone Depletion Potential). The old refrigerants can be referred to as HFC's (hydrofluorocarbons) or CFC's (Chlorofluorocarbons) which indicates their chemical structure contains hydrogen, fluorine, chlorine and carbon. The GWP of a refrigerant released in the atmosphere is measured relative to carbon dioxide, which has a GWP of 1. Carbon dioxide contributes to the global warming by absorbing infrared radiation emitted by the earth's surface, which would otherwise be emitted to space. Thus releasing one molecule of R407C which has a GWP of 1530 corresponds to releasing approximately 1530 carbon dioxide atoms in the atmosphere [7]. The ODP is measured relative to trichlorfluormethan which has an ODP of 1. Refrigerants with a long life time, will at some point reach the upper atmosphere when released. When the refrigerant breaks down and releases chlorine it further reacts and breaks down the ozone molecules. The ozone molecules protects against the ultraviolet radiation from the sun, which can cause skin cancer. R407C do not contain any chlorine atoms and its ODP is therefore 0. As for now, refrigerants are phased out by both national and international regulations. In Denmark, Norway, Sweden and Spain subsidies as an incentive for using low GWP refrigerants has be introduced while HFC refrigerants has been imposed a taxes. In addition to this, forced regulations could occur in the future in order to reduce the consumption of HFC's and other currently used refrigerants. [8] [9]

As mentioned the refrigerant used for the prototype system is R407C which is a mixture of other refrigerants. R407C consists of R134a (52%), R125 (25%) and R32 (23%) and is a zeotropic mixture since each of the compounds has different boiling points [7]. This results in a temperature glide during condensation and evaporation as seen in fig. 2.6.

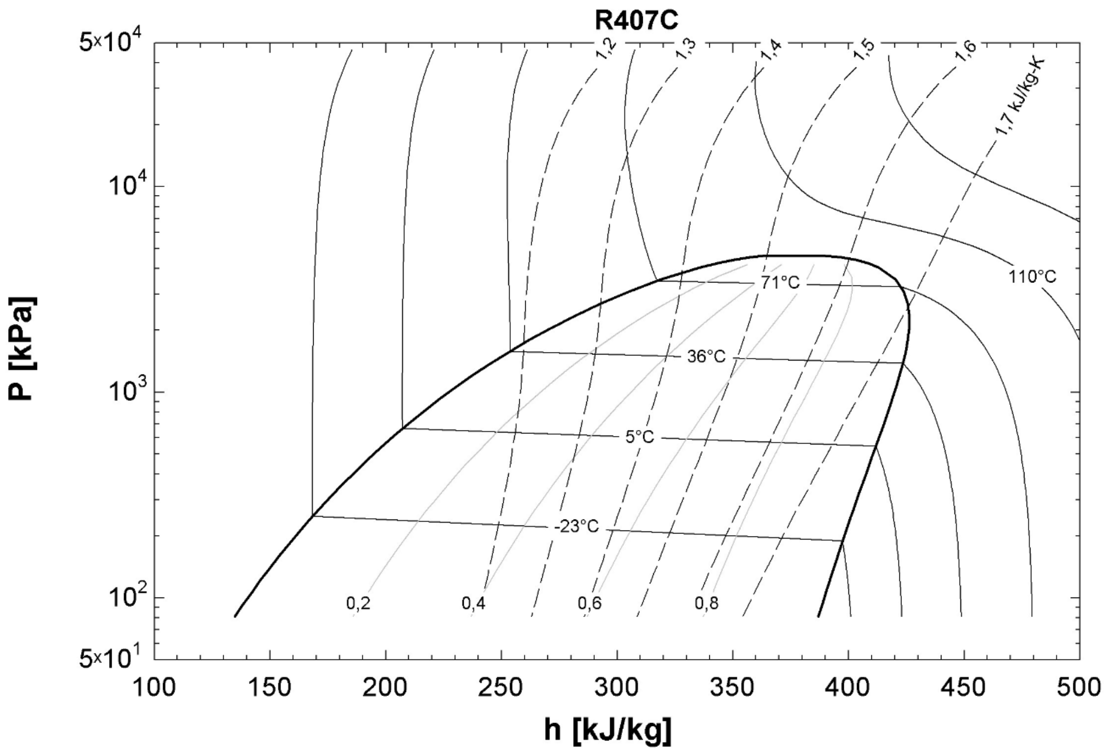

Figure 2.6. Log Ph-diagram for R407C showing a temperature glide within the vapor dome.

In fig. 2.6 the lines indicating a constant temperature are inclined within the vapor dome. When utilizing refrigerants in combination with AHU's the affect of leakages should be carefully considered. Some refrigerants can be flammable from which a spark from a fan could cause a fire or an explosion. Other refrigerants are toxic from which leakages could cause severe health risks in occupied buildings. To eliminate these risks, the heat pump system with be implemented within an isolated cabinet attached to the AHU. Within the cabinet the evaporator, condenser and compressor will be mounted. Future refrigerants are being developed to replace the old HFC's such as R407C. The thermophysical properties of the new refrigerants should however be identical to the old ones in order to achieve similar performance of a heat pump system. The development of new replacements for the old refrigerants usually comes with trade-offs. The old CFC's and HFC's are non flammable and has a low toxicity, the trade-offs are a high GWP and ODP. A natural refrigerant such as ammonia is highly toxic but is often used for industrial applications due to a high heat capacity. Another natural refrigerant with a future potential is CO_2 (R744) since it has a GWP of 1 and a high density. [8] [10]

The toxicity and flammability of refrigerants are divided in to different classes according to the ASHRAE (American Society of Heating, Refrigerating and Air-conditioning Engineers) standards as seen in fig. 2.7.

Flammability ↑ / Toxicity →	Lower Toxicity	Higher Toxicity
No flame Propagation	**A1:** CFC, HCFC, most HFCs	**B1:** Seldom used
Lower Flammability	**A2L:** Most HFOs, R32	**B2L:** Ammonia
Flammable	**A2:** R152	**B2:** Seldom used
Higher Flammability	**A3:** Hydrocarbons	**B3:** no refrigerants

Figure 2.7. Refrigerant flammability and toxicity according to the ASHRAE standards. [8]

In fig. 2.7 it can be seen that refrigerants with low flammability and toxicity are denoted class A1 while refrigerants with high flammability and toxicity are denoted class B2. The new upcoming replacements for the old common refrigerants R134a, R404A, R410A and the R407 series can be seen in fig. 2.8. The new replacements shown in fig. 2.8 are colored by a grey or red colour indicating the flammability and toxicity accordingly to the AHSRAE standards. It can be seen that the disadvantage of utilizing the low GWP replacements are an increased flammability. The HFO's (Hydrofluoroolefins) refrigerant such a R1234ze are a new type with a very low GWP, these could also have a great potential for future heat pump applications.

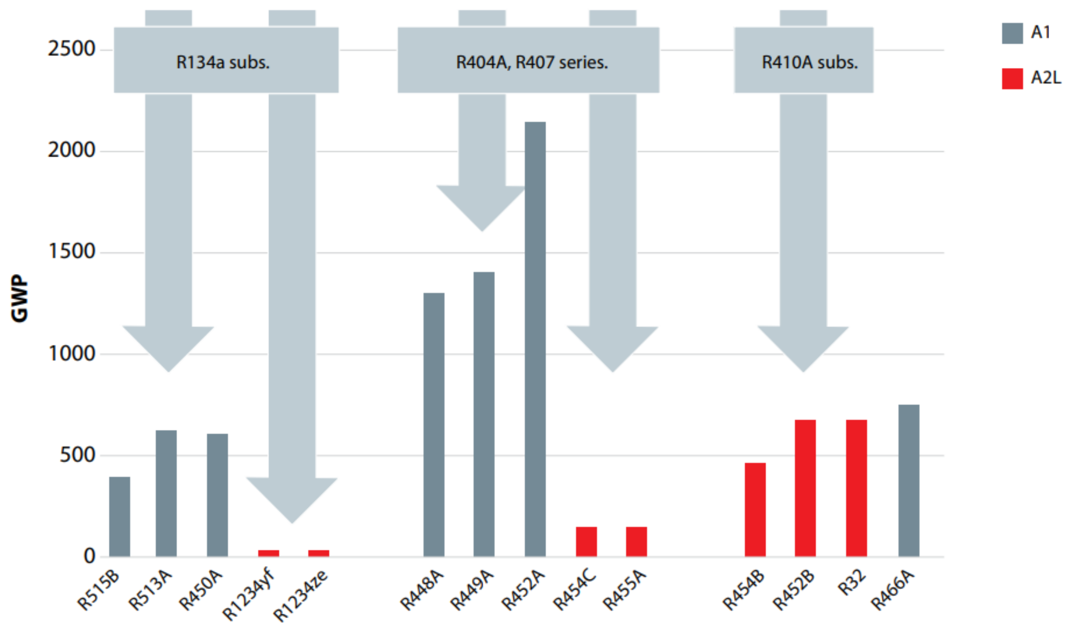

Figure 2.8. Future replacements for old refrigerants, their GWP and ASHRAE classification. [8]

Compressor Analysis and System Configuration

The compressor suggested by Danfoss for the application is called VTZ215-G and is a reciprocating compressor, the data sheet can be found in app. A on page 63. The compressor has four cylinders which each has a swept volume of $215\,\mathrm{cm}^3/\mathrm{rev}$. The VTZ215-G and and the frequency controller can be seen in fig. 2.9.

Figure 2.9. Illustration of the reciprocation compressor VTZ215-G and the VLT. [11]

An illustration of a reciprocating compressor cylinder can be seen in fig. 2.10. The suction side from which the vaporized refrigerant enters the compression chamber can be seen at point **(1)**. As the piston at point **(4)** withdraws the suction valve opens and the refrigerant enters the cylinder. During a compression in the cylinder the discharge valve at point **(2)** will open as the pressure within the cylinder increases. The compressed refrigerant will finally be released through the discharge side at point **(3)**.

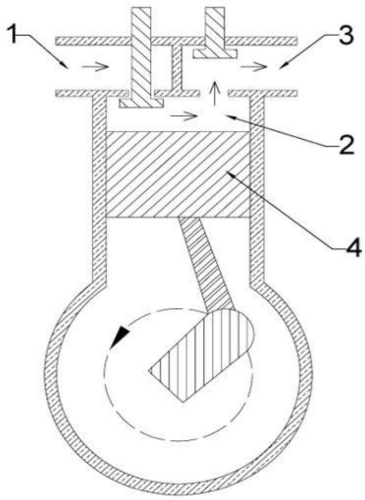

Figure 2.10. Illustration of a reciprocation compressor cylinder. [12]

In order to reduce the wear of the piston and moving parts within the compressor, an oil is mixed together with the refrigerant for lubrication. The VTZ215-G compressor has a maximum cooling capacity of 63.5 kW while running at 90 Hz as seen in app. A on page 63. The required cooling capacity during a worst case scenario is approximately 115 kW which is twice the amount that can be provided by the compressor. By utilizing the software CoolSelector developed by Danfoss, an alternative compressor for the system can be suggested. The software can select compressors based on the desired refrigerant type, cooling capacity, condensation temperature and evaporation temperature. Based on these parameters the software suggested a scroll compressor called SY380-4 which has a maximum cooling capacity of 122.8 kW at 60 Hz. The data sheet for SY380-4 scroll compressor can also be seen in app. A on page 63. A scroll compressor is composed of two metal scrolls as seen in fig. 2.11 which makes up the compressor cylinder. One of the scrolls is stationary while another is orbiting around the stationary scroll. The refrigerant enters at the outer section of the scrolls and as the scrolls rotates the refrigerant is compressed towards the center from which it will be discharged.

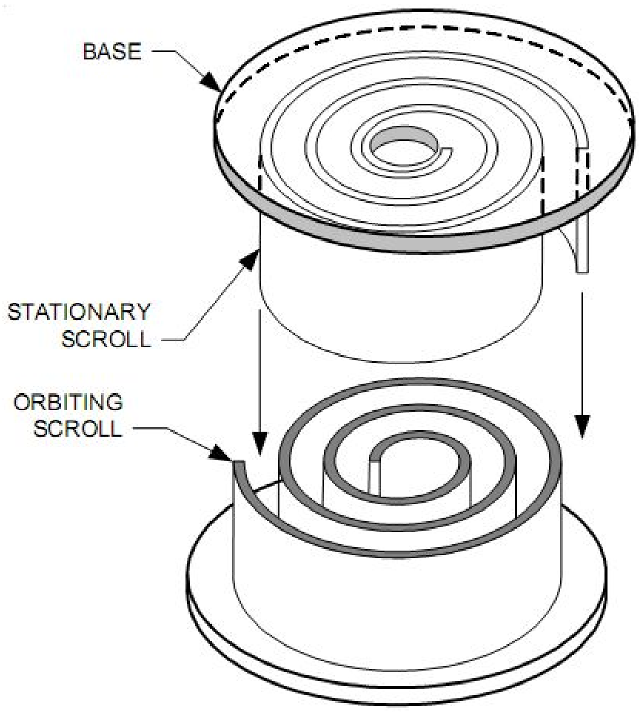

Figure 2.11. Illustration of a scroll compressor cylinder. [13]

The SY380-4 compressor can not be controlled through a VLT to adjust the cooling capacity, therefore the compressor operates at a fixed frequency of either 50 or 60 Hz. Based on the selected frequency, the cooling capacity is affected by the temperature of the condenser and evaporator as seen in the SY380-4 data sheet in app. A on page 63.

Since both compressors presented in this section cant provide the desired requirements in terms of control or cooling capacity a solution could be to utilize both compressors in different configurations. The control and cooling capacity can be achieved by utilizing two vapor compression cycles coupled in series as seen in fig. 2.12. For a system seen in fig. 2.12 with two VTZ215-G compressors, the maximum cooling capacity of 63.5 kW can be supplied over two cycles. As a result two VTZ215-G compressors can provide a total cooling capacity of 127 kW and also be controlled accordingly to the cooling demand through the VLT. The disadvantage of implementing the system is that twice the components are required which affects the capital expenditures (CAPEX). Furthermore an issue is also that the system takes up more space within the AHU.

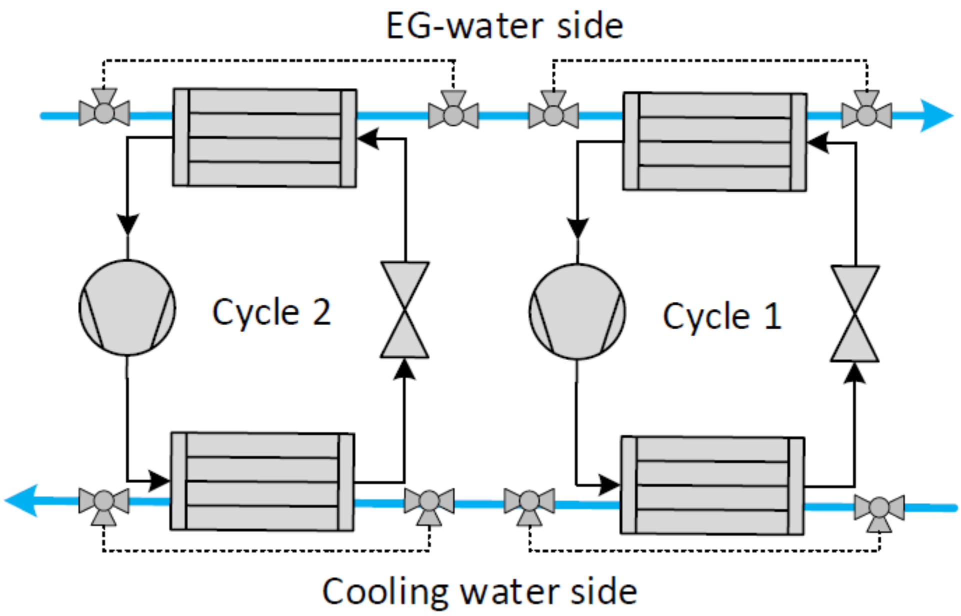

Figure 2.12. Dual cycle system operating in cooling mode.

The system performance could be increased by using the dual cycle design since the temperature difference between the evaporator and condenser is lowered when cooling in intervals throughout two cycles. This improves the COP (Coefficient of Performance) of the system since less work is required for pressurizing the refrigerant. The system cost can be reduced by using a fixed speed compressor in cycle 2 and a VLT compressor in cycle 1, since compressors without a VLT are less expensive.

In cycle 1 the VLT compressor will adjust accordingly to the cooling demand until the maximum cooling capacity of 63.5 kW is reached. Cycle 2 then activates using a fixed speed compressor providing a constant cooling capacity of e.g. 63.5 kW. As cycle 2 activates the VLT compressor in cycle 1 will shut off until the required cooling capacity exceeds 63.5 kW. When the required cooling capacity exceeds the limit of the fixed speed compressor the VLT compressor will activate again and provide additional cooling above 63.5 kW. If the required cooling capacity was 80 kW then compressor in cycle 2 will provide 63.5 kW and the VLT compressor in cycle 1 the last 16.5 kW. The system configuration as seen in fig. 2.12 is generally a result of the compressors available on the market can not provide enough cooling for the system. Danfoss are currently developing compressors for this purpose which uses HFO refrigerants, however these will firstly be available by 2022.

An alternative to the system seen in fig. 2.12 on the facing page could be to utilize a hybrid manifold developed by Danfoss, which connects two compressors in parallel as seen in fig. 2.13. To control the cooling capacity and achieve the desired cooling this system also uses a VLT compressor and a fixed speed compressor. The benefit of using this system is that it only requires one cycle and therefore only one condenser and evaporator. [14]

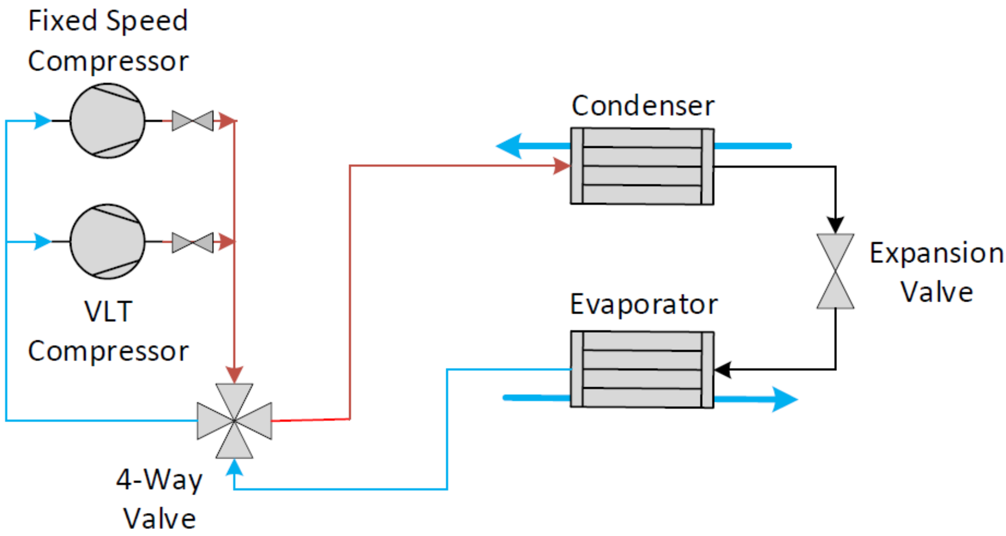

Figure 2.13. Single cycle system with parallel coupled compressors.

A disadvantage of using the parallel compressor system compared to the dual cycle system is that the system reliability is lower. If a compressor breaks down the whole system will shut down, however for the dual cycle system it can still operate at half capacity. Another issue for the parallel system is that the oil should be distributed equally between the two compressors. For a system seen in fig. 2.13 oil can be trapped in the non-active compressor, evaporator, condenser or the tubes. In order to prevent that the oil is getting trapped, both compressors have an oil-sensor which can ramp up the flow for a short period if a low oil level is measured. [14]

Analysis of Evaporator and Condenser Heat Transfer

The heat exchangers used for the system will be chosen through a software provided by Danfoss called Hexact. By utilizing the software, the condenser and evaporator can be designed based on the mass flows, inlet quality, evaporating temperature or condensing temperature. For the system it will be desired to increase the size of the heat exchangers such that the pressure losses are reduced and the operational expenditures (OPEX) lowered. In order to gain a better understanding of the important parameters when designing a condenser and evaporator the heat transfer process will be explained.

As heat is transferred during condensation or evaporation process the flow can be divided in to different regimes. The regimes throughout an evaporator can be seen in fig. 2.14 and consists of a boiling regime and a superheated regime.

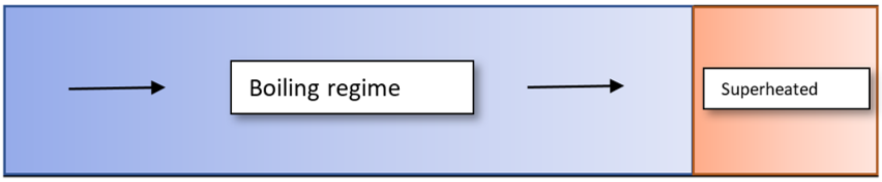

Figure 2.14. Illustration of the regimes through an evaporator.

When the refrigerant enters the evaporator it is a mixture of vapor and liquid from which the inlet quality, x, will be approximately 0 to 0.3. Since the refrigerant is a zeotropic blend of three compounds the compound with the lowest boiling point will firstly evaporate. As the refrigerant evaporates energy is extracted from the secondary fluid in the heat exchanger, corresponding to the enthalpy of vaporization multiplied by the mass evaporated. The enthalpy of vaporization, h_{fg} is a function of temperature and pressure and during evaporation energy is absorbed and during condensation energy is released. The flow type throughout the heat exchanger will also change as the vapor fraction increases, this is referred to as flow boiling. An example of a bubbly flow and stratified flow can be seen in fig. 2.15. The bubbly flow consists of small vapor bubbles which occurs during the beginning of the boiling process. As the vapor fraction increases during the boiling process the flow type changes to a stratified as seen in fig. 2.15. The flow type can be estimated based on the mass velocity denoted G which has the units $\mathrm{kg/m^2 \cdot s}$ and describes the mass flow per cross sectional area of the duct or tube within a heat exchanger. Correlation for flow boiling or condensation, such as the one by Dobson and Chato (1998) which is further described by Nellis & Klein [15], uses the mass velocity as an indicator for the flow type. For a mass velocity $G > 500\ \mathrm{kg/m^2 \cdot s}$ the flow type is assumed annular. For a mass velocity of $G < 500\ \mathrm{kg/m^2 \cdot s}$ the flow is assumed either annular or wavy which is further determined by the Froude number.

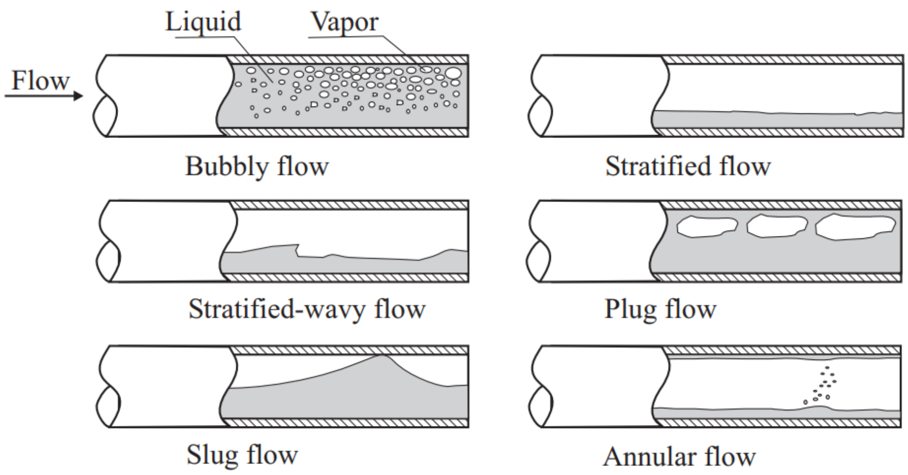

Figure 2.15. Bubbly and stratified flows in horizontal tubes. (edited) [16]

In addition to flow types, different types of flow boiling also occurs which affects the heat flux in the evaporator. The boiling process beings as the surface temperature of the plates within the heat exchanger is greater than the saturation temperature of the refrigerant. In fig. 2.16 the heat flux q'' for a given boiling type can be seen along with illustrations of the flow characteristics. The heat flux q'' is a affected by the temperature difference between the surface temperature T_w and the saturation temperature T_{sat}.

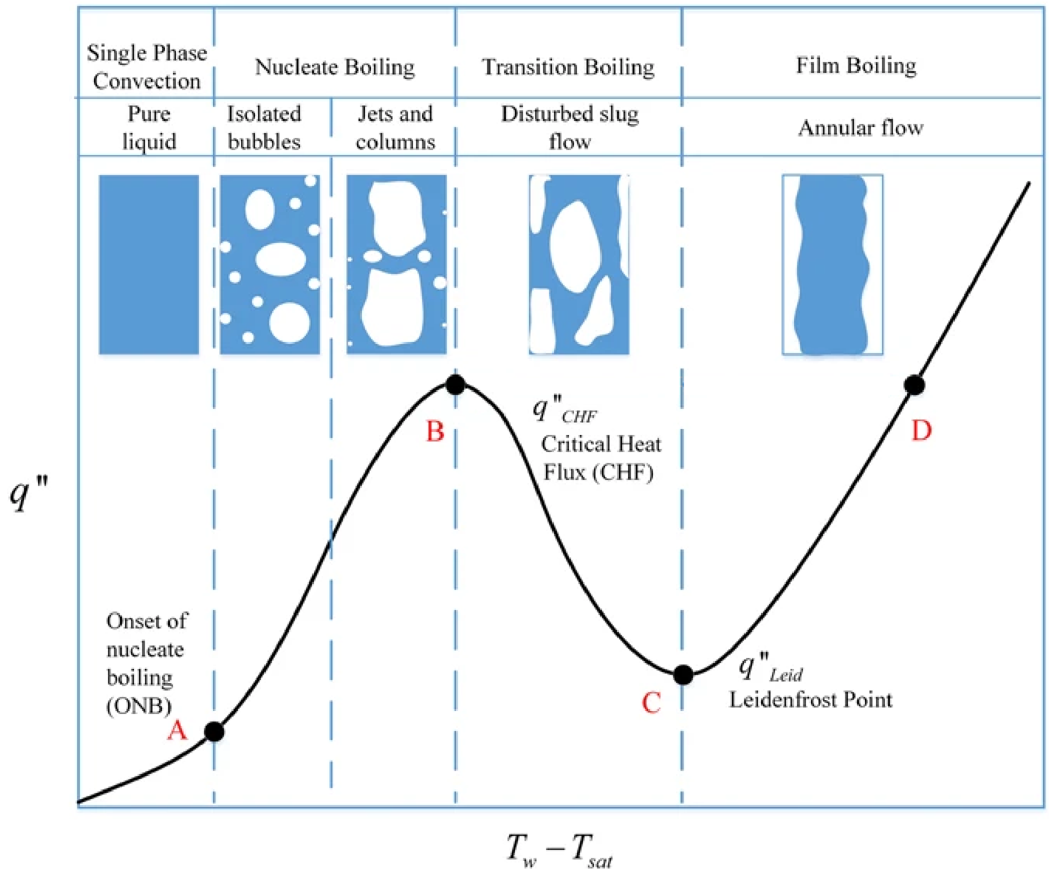

Figure 2.16. Flow and boiling development as the surface temperature increases. (edited) [17]

In fig. 2.16 it can be seen that the heat flux increases from point **A** to point **B** as the temperature difference between the surface and saturation point increases. The maximum heat transfer is reached at point **B** which is also denoted as the critical heat flux. As the surface temperature further increases from point **B** the size of the bubbles increases and acts as an isolation which reduces the heat flux. From point **C** the bubbles begins to form a thin layer covering the surface (Annular flow) and as the surface temperature is further increased towards point **D**, the increase in heat flux is due to increasing radiation heat transfer. [18]

In the superheated region the vaporized refrigerant is heated additional degrees in order to ensure that no liquid enters the compressor chamber. The condenser should not be superheating too much since the primary source of heat transfer should be from the enthalpy of vaporization. Otherwise this results in an oversized and inefficient heat exchanger. As for the evaporator design it is desired to achieve temperature difference between the surface and saturation point such that the critical flux at point **B** is reached.

The condenser can be divided in to three regimes, a de-superheaing, condensing and a subcooled regime as seen in fig. 2.17. After the vaporized refrigerant has been compressed it enters the condenser as a superheated gas in the de-superheating regime. The superheated gas, cools down by heating the secondary fluid side of the heat exchanger through a sensible heat transfer.

Figure 2.17. Illustration of the regimes through a condenser.

Since the surface temperature of the plates within the heat exchanger is lower than the superheated gas it cools down until it reaches the dew point. For a zeotropic fluid the condensation process results in a temperature glide during the condensation process. As for the condensation process two types of condensation can occur a seen in fig. 2.18. To the left dropwise condensation can be seen where vapor condenses on the surface and forms droplets. As the size of the droplets increases the gravity will at some point force the droplets off the surface from which new can be formed. The film condensation can be seen on the right, here a layer of condensed vapor covers the surface. The thickness of the layer increases towards the ground level as gravity affects the film.

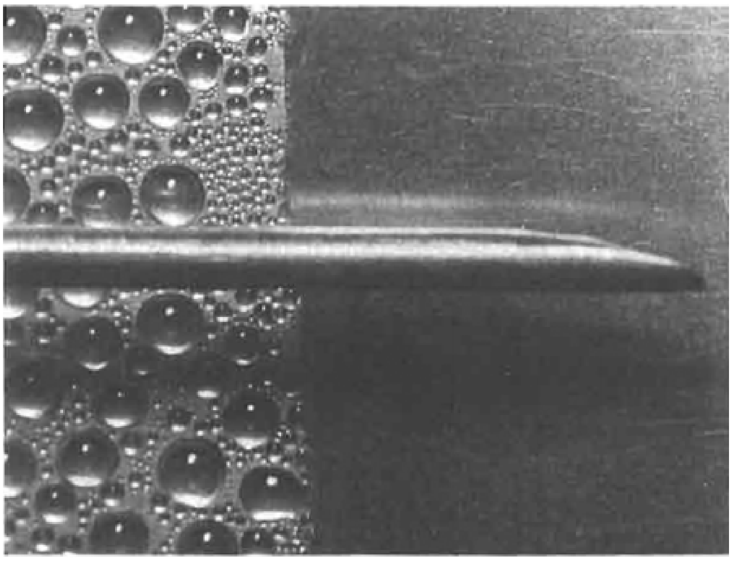

Figure 2.18. Illustration of the dropwise and film condensation. [19]

As all the vapor has condensed the subcooled regime begins, from which the liquid refrigerant is subcooled typically a few kelvin below the condensing temperature before it flows to the valve.

The maximum cooling during a worst case scenario for the evaporator is approximately 115 kW and the maximum heat demand for the condenser is 90 kW. For the condenser and evaporator it is important that the refrigerant flow can reverse while the brine-flows (Cooling water and EG-water) remain the same direction. As a result of this, the condenser and evaporator will run as a counter-current heat exchanger in cooling mode and a co-current heat exchanger in heating mode.

The average temperature profile through a counter-current heat exchanger is higher than a co-current during sensible heat transfer. As a result the heat transfer through a co-current heat exchanger is lower compared to a counter-current. As for a counter-flow heat exchanger it provides a more uniform temperature distribution through the heat exchanger. This results in an average higher temperature difference, which makes the counter-current preferred for sensible heat transfer. However, in a condenser and an evaporator where a phase change occurs the temperature will remain constant, assuming no pressure losses. The temperature profile during condensation and evaporation with no subcooling, superheating or de-superheating can be seen in fig. 2.19.

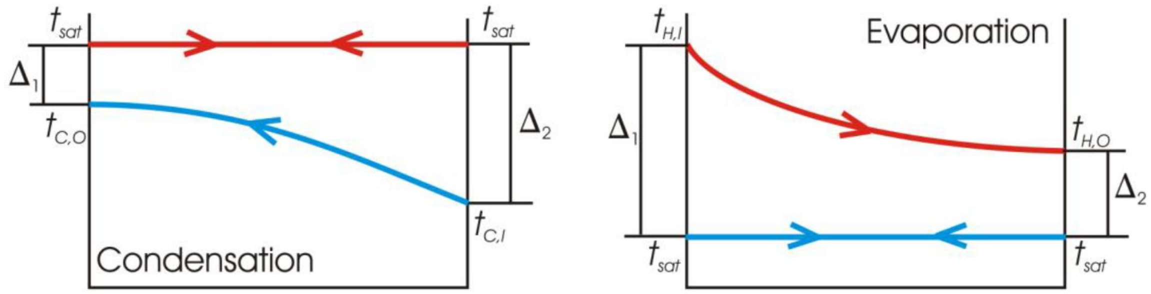

Figure 2.19. Temperature profiles during latent heat transfer. [20]

Here, it can be seen that the only the secondary fluid changes temperature, while the refrigerant keeps a constant temperature during the phase change. However, since the same amount latent energy is emitted/absorbed regardless of the direction, the temperature profile of a counter-current or a co-current heat exchanger will be identical.

2.4 Weather Data Analysis and Operating Hours

The plan is to build a prototype system located in Neumünster, however the closest available weather data provided by Danfoss is for Frankfurt. The two location are approximately 500 km apart and both has an oceanic climate which generally results in small temperature variations. In the factory it is desired to maintain a temperature of 22 °C to 23 °C during both winter and the summer. The main purpose of the system during the summer is to remove moist content from the air during days with high relative humidity and temperatures. In the winter, the system only heats up the air when the heat recovery of the double cross flow heat exchanger is not sufficient. The means that the system will only operate a certain amount of hours during the year, where dehumidifying, cooling and heating is necessary.

An important aspect to consider is that the system is to be implemented at Danfoss factories in the U.S. which are exposed continental climate. As a result, the air temperatures fluctuations are more extreme and ranges from −21 °C to 37 °C throughout the year and generally has a higher moist content based on weather data for Ames provided by Danfoss. Comparing it to the German weather data, the required energy for cooling and heating in Neumünster is generally lower which results in fewer operating hours. In addition to that, the system has to work within a lower temperature span which lowers the operating requirements for the components. In fig. 2.20 the dry bulb temperature in Frankfurt, throughout the hours of a year starting from 1st of January can be seen.

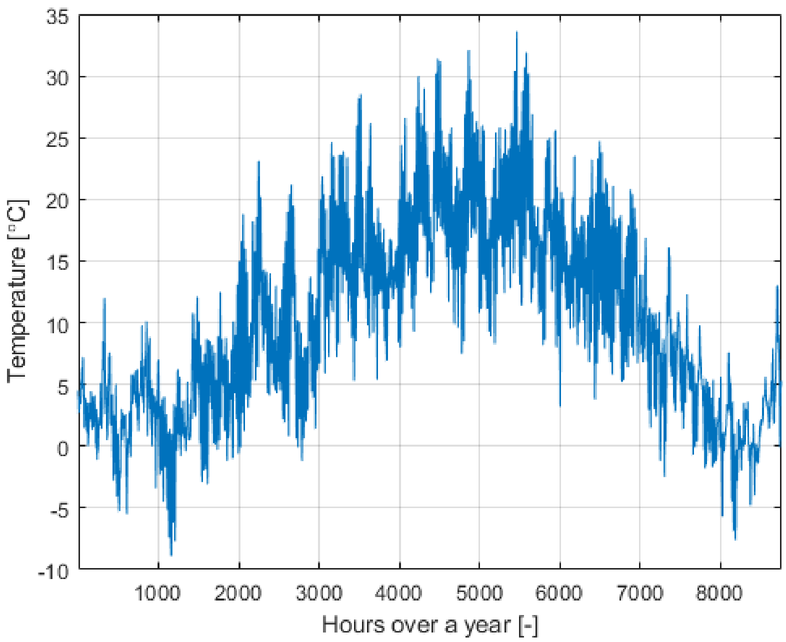

Figure 2.20. Dry bulb temperature throughout a year in Frankfurt.

Here it can be seen that the temperature in Frankfurt ranges from −7 °C to 34 °C throughout the year. Since the temperature within the factory is the be kept at around 22 °C to 23 °C, it can therefore be seen that primary function of the system is to heat since majority of the hours are at a temperature below 10 °C.

Since the amount of energy required for cooling is affected by the moist content, this aspect should also be considered. The relative humidity throughout the year in Frankfurt can be seen in fig. 2.21. Here it can be seen that the relative humidity drop during the summer, which is a result of the warmer air. Since hot air can contain more moist content than cold air, the relative humidity is generally higher during winter and lower in the summer. It can also be seen in fig. 2.21 that as the temperatures increases during summer, the relative humidity drops.

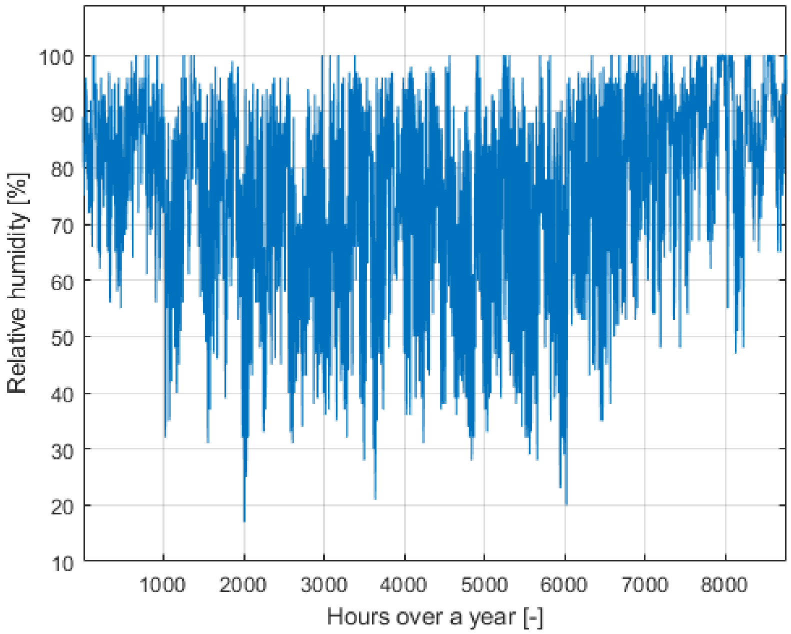

Figure 2.21. Temperature profiles during latent heat transfer.

The moist content in the air can be described by the humidity ratio, ω, which describes the kilogram of moist per kilogram of air. The humidity ratio is a function of the air pressure, relative humidity and temperature. The humidity ratio will be used to describe amount of moist removed over the cooling coil. In regards to the required relative humidity of the factory have not set any specific requirements. However, it is generally desired to have a low humidity in buildings in order to avoid fungus or material damage. Furthermore for the people who is occupying the building a high humidity and temperature can also lead to discomfort.

2.5 Problem Statement

As described in chap. 1 on page 1, the global carbon emissions has increased rapidly throughout the last century. Industrial processes are a major contributor to the carbon emissions due to the consumption of fossil fuels used for heating and cooling in factories. As a result there is an increased focus on resolving this through a green transition. Through the implementation of a heat pump systems which is coupled to the cooling water network in factories, excess energy from production could be use to both heat and cool ventilation air. Based on this low COP rooftop chillers and gas furnaces can be replaced from which both a carbon neutrality and energy optimization could be achieved. The system could therefore have a future business potential from which companies like Danfoss can save money through energy optimizations of factories and also make them carbon-neutral. In order test such a system, Danfoss and NB-ventilation has entered in to a collaboration in order to build and test a prototype. If the prototype which is to be implemented in Neumünster can achieve good performance in terms of COP and repayment period it could have a major business potential for both NB-ventilation and Danfoss. The main objective of this study is to model the heat pump system which is described in sec. 2.1 on page 3. Based on the chosen components for the application, the model should be able to provide the performance of the system as a function of the ambient temperatures. Furthermore, based on the performance of the system, an economical analysis should be made which can estimate the CAPEX, OPEX and the repayment period.

How can a heat pump system which is coupled between a cooling water network and an AHU be modelled and the performance be determined?

- How can a cooling tower and a double cross flow heat exchanger be modelled?
- How can weather data be utilized in order to design the heat pump system?
- How can the CAPEX and OPEX be estimated in order to determine the repayment period?

System Modelling 3

In this chapter the process of developing a model which can determine the performance of the heat pump system will be presented. Furthermore, the assumptions and choice of components will also be reviewed. The objective of the model is to describe the performance of the heat pump system described in sec. 2.1 on page 3 based on weather data inputs. The system will be modelled using EES (Engineering Equation Solver), which is a non-linear equation solver, from which thermophysical properties of fluids are available. The model includes the following components which are a condenser, an evaporator, a compressor, a cooling tower, a double cross flow heat exchanger, a cooling and heating coil. For simplicity, the heat pump system in the model is assumed to only consist of a single vapor compression cycle and not as the systems configurations presented in 2.3 on page 7. The air flow in the AHU is 20,000 m^3/h and the maximum energy requirement for cooling and heating is 115 kW and 90 kW. The components used for the model are generally based on real Danfoss components which are available on the market, from which data sheets can be used for the model. Since the exact components are known this can provide a good economical analysis for both the OPEX and CAPEX.

3.1 Modelling of the Compressor

As described in sec. 2.3 on page 7, the compressor suggested by Danfoss uses a VLT, however with a maximum cooling capacity of 63.5 kW it cannot be utilized for the system since it is too small. Therefore the SY380-Y compressor without a VLT was chosen for the model since it can provide a cooling capacity of 122.8 kW. In order to adjust the capacity of a compressor the VLT would normally send a 0 V to 10 V signal from which the RPM (Rounds per minute) are adjusted. As seen in eq. 3.1 the RPM directly affects the mass flow of the system, here η_{vol} is the volumetric efficiency, ρ_v is the compressor inlet density and V_{swept} is the swept volume of the compressor.

$$\dot{m} = \frac{n_{RPM}}{\frac{60 \cdot s}{min}} \cdot \eta_{vol} \cdot \rho_v \cdot V_{swept} \tag{3.1}$$

Since the compressor has no VLT, the RPM will be locked at 3600 RPM ($\approx$ 60 Hz) however the heating and cooling capacity will be adjusted through the condensing and evaporating temperature. In the model, the mass flow of the refrigerant will be found by making a lookup table based on parameters from the SY380-Y data sheet found in A on page 63. Based on the table, the model can provide the mass flow, power consumption, volumetric efficiency, cooling and heating capacity through interpolation. The data points will be interpolated using a bi-quadratic method from which a value is found by utilizing the 16 closest data points. In the table, two independent values, which are the evaporation and condensing temperature are chosen to describe a third, which is either the mass flow or compressor power of the system.

The condensing and evaporation temperature will be a function of the cooling water and EG/water flow outlet temperature in the condenser and evaporator. The temperatures are chosen such that no temperature crossings will occur in the evaporator and condenser. This done by setting the condensation temperature equal to the outlet flow temperatures and adding or subtracting 5 K. In 'Cooling Mode' the condensing and evaporating temperatures are defined as seen in eq. 3.2 and 3.3.

$$T_{cond} = T_{CW,out} + 5K \tag{3.2}$$

$$T_{evap} = T_{EG,out} - 5K \tag{3.3}$$

Here, $T_{CW,out}$ is the outlet temperature of the cooling water and $T_{EG,out}$ is the outlet temperature of the brine (EG/water). Since the vapor compression system reverses for 'Heating Mode' the temperatures will be defined as seen in 3.4 and 3.5.

$$T_{evap} = T_{CW,out} - 5K \tag{3.4}$$

$$T_{cond} = T_{EG,out} + 5K \tag{3.5}$$

The $\pm 5K$ are used as a safety factor which ensures the refrigerant's evaporating or condensing temperature is always above or below the secondary fluid side in the heat exchanger. Based on the lookup tables made from the data sheets, the model can now describe the characteristics of the SY380-Y compressor. From which the mass flow and compressor power can be determined based on interpolation of the data sheet.

3.2 Modelling of the Condenser and Evaporator

Based on conversations with Danfoss, the heat exchanger type H118-E, which is optimized for R407C refrigerant was chosen for the system. The evaporator and condenser will be modelled based on data from a Danfoss software called Hexact. The program can determine the heat transfer of the condenser and evaporator based on the mass flow, inlet quality, evaporating or condensing temperature. The model will be based on the assumption that there is no pressure loss over the condenser and evaporator. The system will operate as counter-current in both 'Heating Mode' and 'Cooling Mode'. In the condenser and evaporator it is assumed that all the refrigerant is condensed and evaporated. For the evaporator the refrigerant inlet quality is assumed to be 0.25 and the superheating is assumed to be 3 K. For the condenser the inlet temperature is assumed to be 5 K above the condensation temperature and the subcooling is assumed to be 3 K.

In order to model the condenser and evaporator, lookup tables was made in EES similar to the one of the compressor by utilizing Hexact. In Hexact, parameters such as mass flow of the refrigerant and the evaporating temperature was varied in order to determine the load at different operating conditions. The parameters which Hexact uses to calculate the evaporator performance can be seen in fig. 3.1. Here it can be see that the calculations are based on a counter-current H118-E plate heat exchanger with 100 plates. For the brine side the mass flow was selected based on operating mode of the system. For 'Cooling Mode' the evaporator was connected to the EG/Water side from which the mass flow is 3,792 kg/s. For 'Heating Mode' the evaporator is connected to the cooling water from which the mass flow is 4 kg/s.

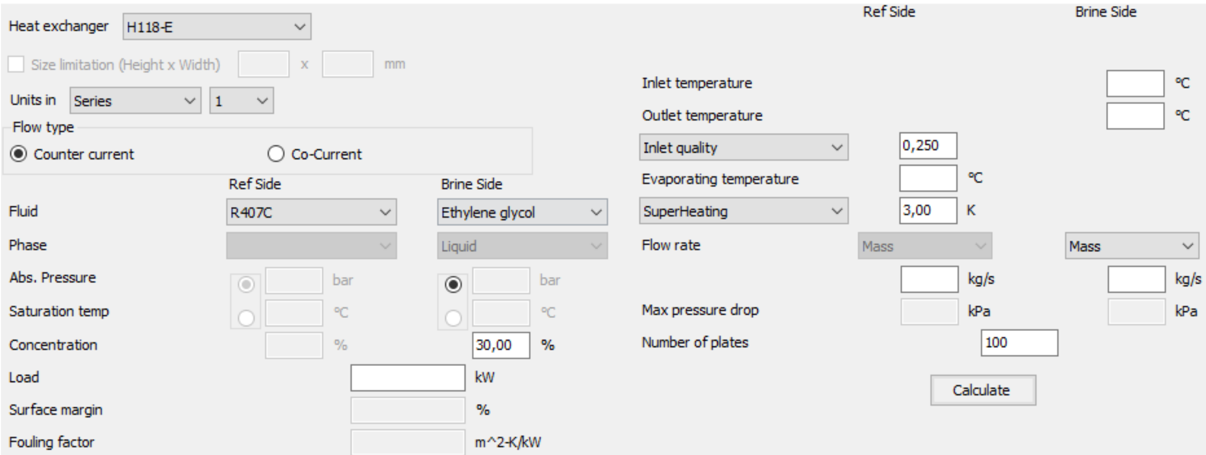

Figure 3.1. Hexact parameters for an evaporator

To describe the load of the evaporator the mass flow was varied from 0.1 kg/s to 1 kg/s and the evaporating temperature was varied from −17.5 °C to 17.5 °C. For the condenser, the mass flow was varied from 0.1 kg/s to 1 kg/s and condensing temperature from 40 °C to 65 °C. By entering the results of the cooling or heating load in a table in EES, the performance of both the condenser and evaporator can be described as a function of mass flow and temperature. This is done by interpolating the table values in EES through a bi-quadratic method, as it was done for the compressor model. The condenser and evaporator uses the evaporating- and condensing temperature and the mass flow calculated by the compressor model as an input. From this the heating and cooling load of the H118-E heat exchanger model can be described.

Since the condensing and evaporating temperature is based on the outlet temperature of the cooling water and EG/Water mixture, these has to be defined through an energy balance. An illustration of the heat transfer between the EG/Water mixture and the refrigerant during cooling and heating mode can be seen in fig. 3.2. Here the blue arrow indicates the removal of heat, *Qevap*, in the EG/Water flow during evaporation. The red arrow indicates the addition of heat, *Qcond*, to the EG/Water flow during condensation.

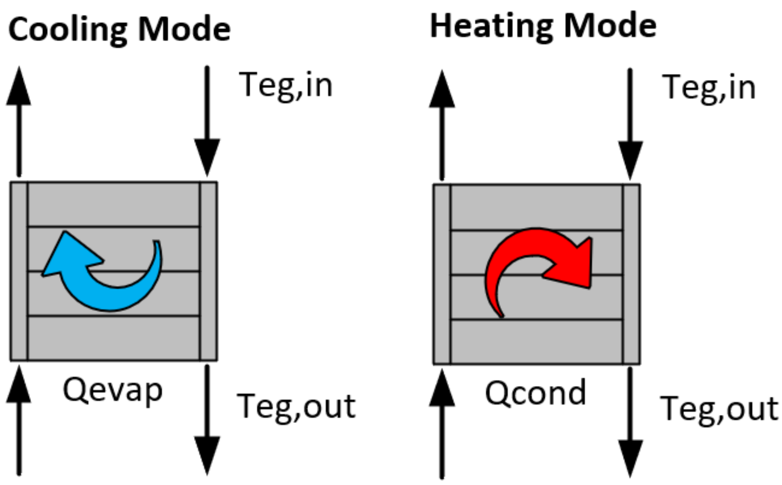

Figure 3.2. Heat transfer of the EG/Water flow during "Cooling Mode" and "Heating Mode".

Since the heat load of the evaporator, *Qevap* and the condenser *Qcond* can be determined through interpolation, the outlet temperature can be calculated by defining the inlet state of the EG/Water flow. In order for the EG/water to be affected by the outside temperature, it is assumed that the inlet temperature of the EG/Water mixture is equal to the inlet temperature of the cooling water. The inlet temperature of the cooling water is directly affected by the outside temperature, the calculation will be further described in sec. 3.5 on page 30. The energy balance has to be defined for both "Heating Mode" and "Cooling Mode", since energy is either removed or supplied. The energy balance for the EG/Water flow during "Heating Mode" is defined in eq. 3.6. The energy balance for the EG/Water flow during "Cooling Mode" is defined in eq. 3.7.

$$\dot{Q}_{EG,out} = h_{EG,in} \cdot \dot{m}_{EG} + \dot{Q}_{cond} \tag{3.6}$$

$$\dot{Q}_{EG,out} = h_{EG,in} \cdot \dot{m}_{EG} - \dot{Q}_{evap} \tag{3.7}$$

here, the inlet enthalpy, $h_{EG,in}$, is defined based on two thermophysical properties such as the temperature, $T_{EG,in}$ and a quality of 0. In order to describe outlet enthalpy of the EG/Water flow, $h_{EG,out}$ must be found in order to solve the system of equations. By utilizing eq. 3.8 on the facing page, the outlet enthalpy can be found since $\dot{Q}_{EG,out}$ and $\dot{m}_{EG}$ is already known. The outlet temperature of the EG/Water can then be found by using the two thermophysical properties $h_{EG,out}$ and the quality of the outlet flow. Since no phase change occurs in the EG/Water flow, the outlet quality is assumed to be 0.

$$\dot{Q}_{EG,out} = h_{EG,out} \cdot \dot{m}_{EG} \tag{3.8}$$

The outlet temperature of EG/water mixture can now be determined during "Heating Mode" and "Cooling Mode", based on the heating and cooling loads of the evaporator and condenser.

3.3 Modelling of the Heating and Cooling Coils

The heating and cooling coils should provide additional heating, cooling or dehumidification after the supply air has been processed through the double cross flow heat exchanger. The heating and cooling coils chosen for the system are provided by TT-Coil which is a supplier for NB-ventilation. The coil calculations provided for the system can be found in app. B on page 67. In the model, it is assumed that there is no pressure loss over the coils and the EG/Water mixture used in the coil is assumed to be pure water. The calculations provided by TT-Coil will be used to explain the energy balance of the system in this section. The heat fluxes of the coil circuit during "Cooling Mode" can be see in fig. 3.3. In "Heating Mode" the two coils will operate as a single units which only heats the air 89.3 kW, this can also been seen in the calculations found in app. B on page 67.

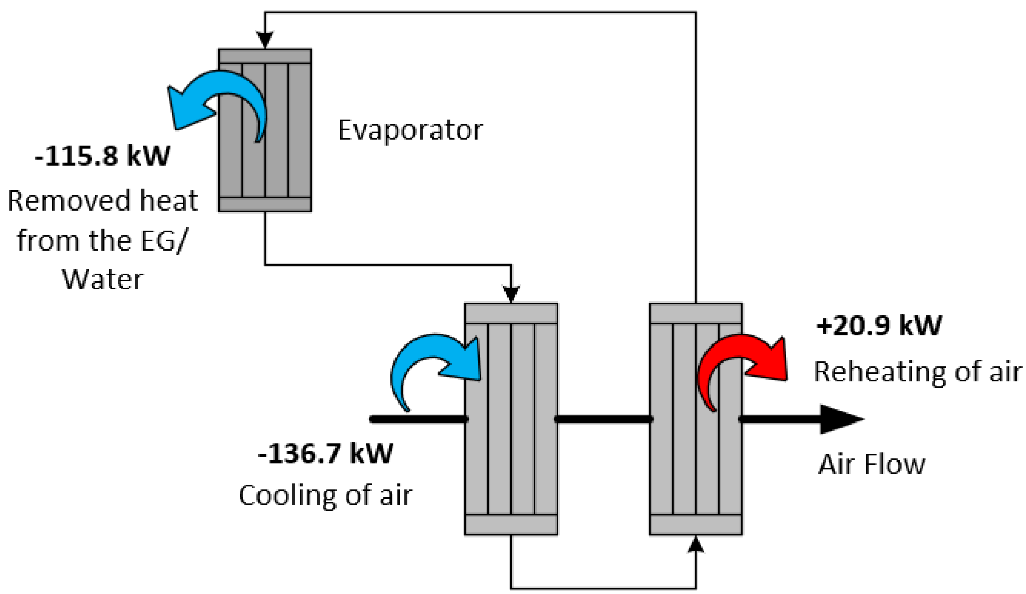

Figure 3.3. Illustration of the energy balance for the EQ/Water circuit during "Cooling Mode".

In fig. 3.3 it can be seen that the air is firstly cooled by removing 136.7 kW, which is absorbed by the EG/Water mixture. As the EG/Water mixture continues through the second coil (After heating coil), the air is heated an additional 3 K after being dehumidified and cooled by the first coil. The system of equations used to describe the energy balance for "Cooling Mode" and "Heating Mode" can be seen in eq. 3.9 to 3.13.

$$\dot{Q}_{evap} = \dot{Q}_{coils} \tag{3.9}$$

$$\dot{Q}_{cond} = \dot{Q}_{coils} \tag{3.10}$$

Here it is assumed that the amount of energy supplied or absorbed by the condenser and evaporator, is equal to the sum of the heat transferred to the supply air through the coils. For simplicity, the model is assumed to only consist of a single cooling coil while operating in "Cooling Mode", from which the after heating coil will not accounted for. While operating in "Heating Mode" the system is also assumed to consist of a single heating coil.

In eq. 3.11 and 3.14 the energy before and after the coils can be calculated. The inlet enthalpy of the supply air, $h_{air,in}$ can calculated since the relative humidity, temperature and ambient pressure is known.

$$\dot{Q}_{air,in} = \dot{m}_{air} \cdot h_{air,in} \tag{3.11}$$

Since $\dot{Q}_{air,in}$ and the heating or cooling load of the evaporator and condenser are known, they can be used in eq. 3.12 and 3.13 to determine $\dot{Q}_{air,out}$.

$$\dot{Q}_{air,out} = \dot{Q}_{air,in} - \dot{Q}_{evap} \tag{3.12}$$

$$\dot{Q}_{air,out} = \dot{Q}_{air,in} + \dot{Q}_{cond} \tag{3.13}$$

Using eq. 3.12 and 3.13, the outlet enthalpy can now be calculated during "Cooling Mode" and "Heating Mode" through eq. 3.14.

$$\dot{Q}_{air,out} = \dot{m}_{air} \cdot h_{air,out} \tag{3.14}$$

Since the outlet enthalpy or the air flow is known, the temperature can be calculated as a function of the enthalpy, humidity ratio and atmospheric pressure.

Mass Balance over the Cooling Coil

When operating "Cooling Mode", the moist content of air is condensed from which a mass balance of the air flow must be defined. Since climate in Frankfurt is not as warm and humid as intended for the system, the effect cooling down the air rarely results in condensation of the moist air. In order to account for this in the model, is assumed that 30 % of the original moist content of the inlet air is always removed over the cooling coil. As the moist air is cooled down throughout the coil, condensate will occur as seen in fig. 3.4, this will be accounted for through eq. 3.16.

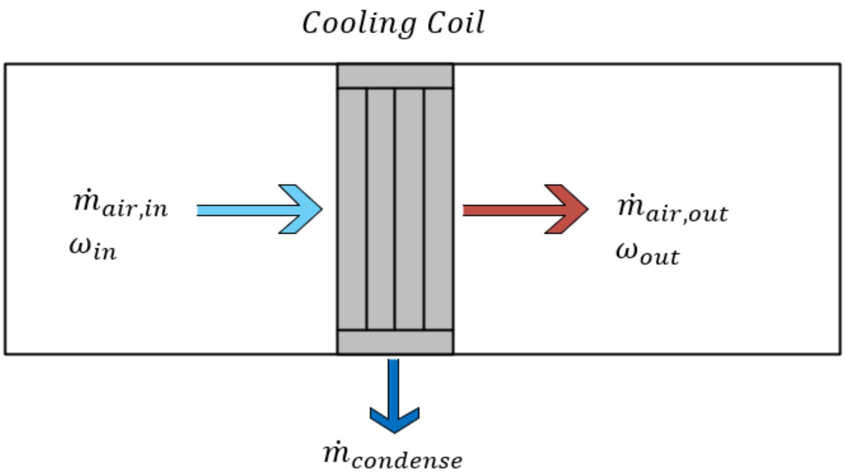

Figure 3.4. Mass flow through the cooling coil.

The mass balance of the air flow over the cooling coil is described through eq. 3.15 to 3.17. Here, $\dot{m}_{air,in}$ is found based on the required volume flow of 20,000 $\mathrm{m^3/h}$ the AHU, multiplied by the air density, $\rho_{air,in}$. The density is found based on the relative humidity, temperature and the atmospheric pressure of the inlet air.

$$\dot{m}_{air,in} = 5.55\,\mathrm{m^3/s} \cdot \rho_{air,in} \tag{3.15}$$

$$\dot{m}_{air,in} = \dot{m}_{air,out} + \dot{m}_{condensate} \tag{3.16}$$

The humidity ratio, ω, represents the amount of water per kilo of air, the amount of moist condensed can therefore be found based on the difference in the humidity ratio over the cooling coil. Since the model is based on the assumption that 30 % of the moist content is condensed over the cooling coil, the outlet humidity can be calculated based on the inlet humidity as seen in eq. 3.17

$$\omega_{out} = \omega_{in} - \omega_{in} \cdot 0.3 \tag{3.17}$$

The amount of condensate can then be calculated from eq. 3.18 since the inlet mass flow of the air and humidity is known.

$$\dot{m}_{condensate} = (\omega_{in} - \omega_{out}) \cdot \dot{m}_{air,in} \tag{3.18}$$

The heat transfer in the coil can be split in to two different segments, a sensible and a latent heat transfer. The sensible heat transfer is the amount of heat used to change the temperature of air, while the latent heat transfer is the amount used to condense the water. In the calculations from TT-Coil, it can be seen that the S.H.R (Sensible Heat Ratio) of the coil is 0.62 which means 62 % of the total 136,7 kW transferred is used to change the temperature. Based on this the remaining 38 % of the total heat transfer is used to remove moist from the air. In order to account for this will be assumed that 40 % of the energy transferred from the evaporator is latent heat and 60 % is sensible heat. The sensible and latent heat transfer can thus be calculated from eq. 3.19 and 3.20.

$$\dot{Q}_{latent} = \dot{Q}_{evap} \cdot 0.4 \tag{3.19}$$

$$\dot{Q}_{sensible} = \dot{Q}_{evap} \cdot 0.6 \tag{3.20}$$

When the system operates in "Heating Mode" the mass balance can be simplified to eq. 3.21 since heating will not result in condensation.

$$\dot{m}_{air,in} = \dot{m}_{air,out} \tag{3.21}$$

This will also result in the inlet humidity ratio is equal to the outlet humidity ratio during "Heating Mode". Based on the energy and mass balances defined in this section, the supply air temperature and relative humidity can now be determined.

3.4 Modelling of the AHU Heat Exchanger

In the system a double cross flow heat exchanger for chosen for recovering heat from the exhaust air. The heat exchanger will process an air flow of 20,000 m^3/h in both the exhaust and supply duct. The reason for choosing a double cross flow is due to a high temperature efficiency of approximately 80 %. Furthermore the double cross flow heat exchanger has no moving parts such as an enthalpy wheel, this can cause a break down of the system. For the heat exchanger model, it is assumed that there is no pressure drop over the heat exchanger. It is also assumed that no condensation occurs within the heat exchanger during cooling of the air streams. The model is based on the calculation for the temperature transfer efficiency, η_{he} which can be seen in eq. 3.22.

$$\eta_{he} = \frac{T_2 - T_1}{T_3 - T_1} \tag{3.22}$$

Here T_1 is the supply air, T_2 is supply after the heat exchanger and T_3 is the exhaust air before the heat exchanger. The temperatures over the double cross flow heat exchanger are also illustrated in fig. 3.5. The exhaust air, T_3 which is leaving the factory will have a temperature of 23 °C, since it is the desired temperature of the factory.

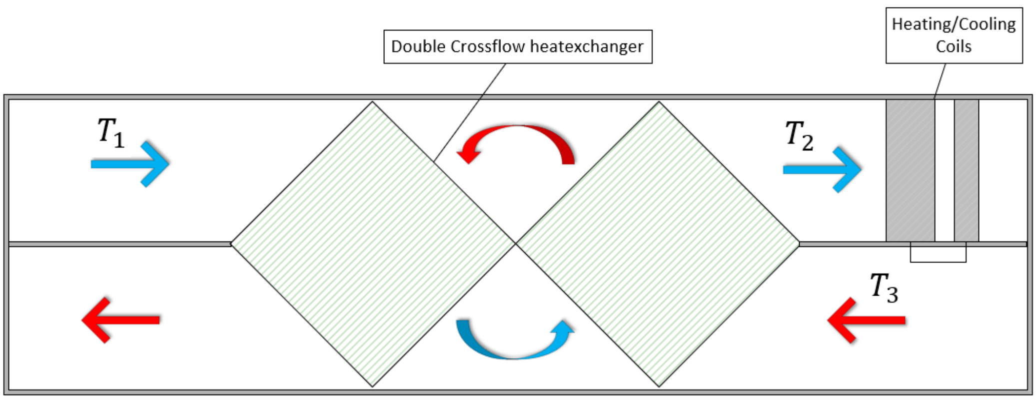

Figure 3.5. Mass flow through the cooling coil.

From eq. 3.22 the supply air temperature after the heat exchanger can be found as a function of the supply air temperature, T_1 and exhaust air, T_3 which will be fixed. Furthermore, by setting temperature efficiency, η_{he} to 80 % which corresponds to a double cross flow, the supply temperature after the heat exchanger T_2, can then be found. This is a simple very simple method of implementing a double cross flow heat exchanger in the model, which processes the air before the heating and cooling coil.

3.5 Modelling of the Cooling Tower

Throughout this study it has been assumed that a cooling tower is implemented as a part of the factory. The exact type of cooling tower has not been selected in this study since it can vary for different factories. In order to model a cooling tower, data has been provided by Danfoss for a Vestas Aircoil cooling tower which can be found in app. C on page 69. The data shows the cooling water temperature as it leaves the cooling tower, for different relative humidities and outside temperatures. Additional the data also provides power consumption for operating the cooling tower which will be used to estimate OPEX. In the data sheet, it can also be seen that the cooling tower do not operate as temperatures drop below 16.8 °C. The cooling tower outlet temperature which is denoted T_{WO} in the data provided, is assumed to be equal to the inlet temperature of the cooling water, $T_{CW,in}$ as seen in eq. 3.23.

$$T_{WO} = T_{CW,in} \tag{3.23}$$

The methodology used to model the characteristics of the compressor, evaporator and condenser will also be used to model the cooling tower. Based on the data provided, a lookup table will be made in EES from which the outlet water temperature of the cooling water and the power consumption can be found. The input for the cooling tower model will be the ambient dry bulb temperature. The data points in the table will be interpolated using linear interpolation.

Modelling Results 4

In this chapter, the results of modelling the heat pump system operating in both "Heating Mode" and "Cooling Mode" will be presented. Furthermore, the method used for processing the weather data, such that the performance under the most often occurring conditions can be found will be explained. Finally an overview of the yearly operating hours of the system will be presented.

4.1 The Bin Data Method

The since the performance of the heat pump system is dependent of the ambient temperature the bin method will be applied. The bin method organizes the temperatures measured over a year into hourly occurrences as seen in fig. 4.1. Here, the red vertical line represents the factory temperature of 23 °C from which it can be seen that majority of hours during the year requires heating. The data in fig. 4.1 can therefore be used as a guidance for designing a system, since it illustrates the most frequently temperature conditions. In order to determine the performance of a system implemented in Frankfurt, the temperatures measured will be used as inputs.

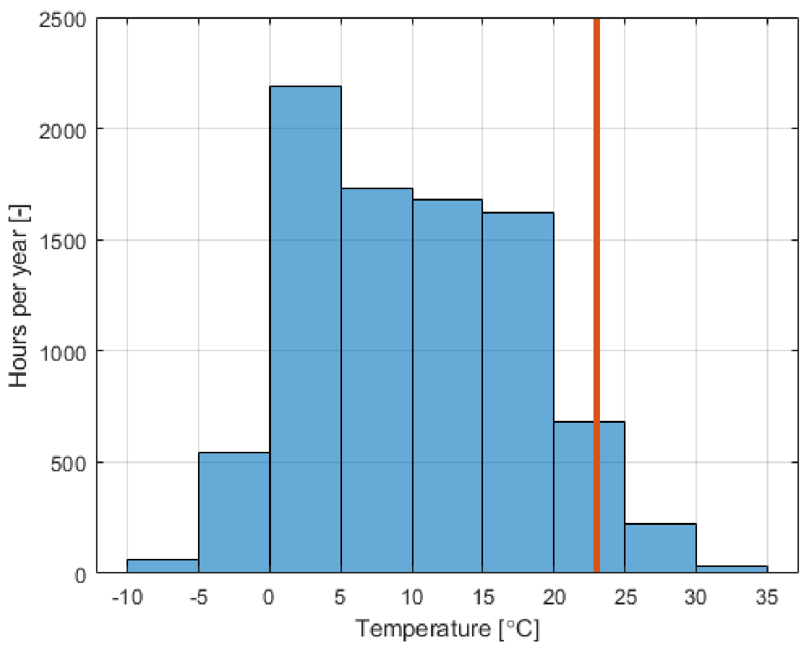

Figure 4.1. Hourly occurrence of the temperatures throughout a year in Frankfurt.

Based on this, the model will provide the performance of each temperature interval, additionally the hourly power consumption at the given condition. The bins in fig. 4.1 on the preceding page covers intervals of 5 °C, to reduce the amount of calculations each bin will correspond to the mean temperature of the interval. For example, the bin covering the interval 5 °C to 10 °C is assumed to have a temperature of 7.5 °C which occurred 1731 hours of the year.

In important aspect to consider is that the system will not operate constantly throughout a year. According to Danfoss, the system begins to cool or heat when the double cross flow heat exchanger can not provide the desired temperature of 23 °C ± 2 °C. However, in the model it is assumed that the system activates "Cooling Mode" for ambient temperature ≥ 25 °C. The system will activate "Heating Mode" for ambient temperature ≤ 10 °C. Based on these criteria the yearly hours can be seen in fig. 4.2.

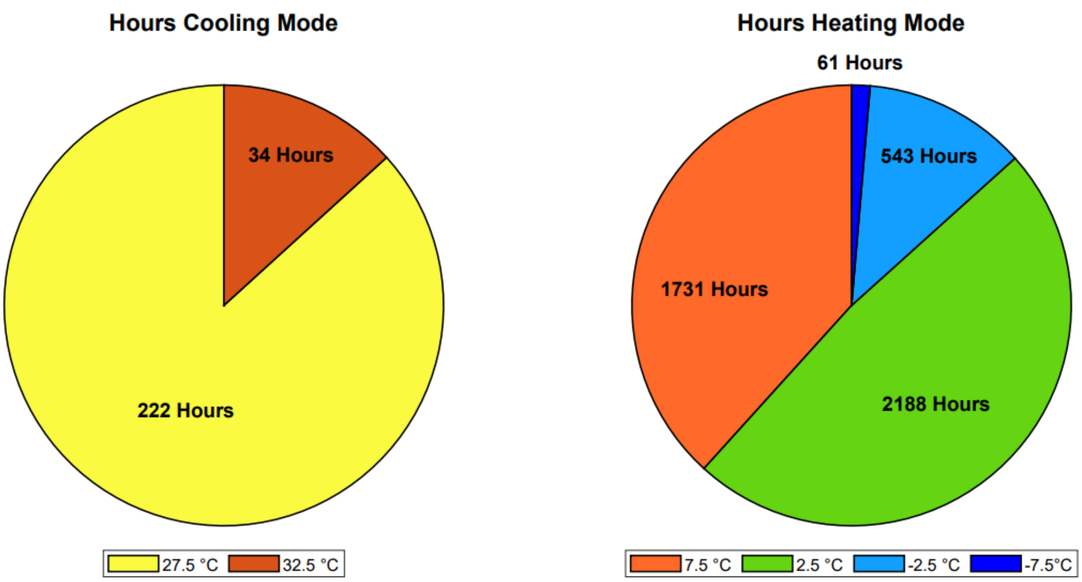

Figure 4.2. Pie chart of the yearly cooling and heating hours.

By summing up the operating hours from fig. 4.2, it was found that the system will operate 4,779 hours yearly. The general performance of the system will be found by using the temperature intervals as inputs for the model. The relative humidity of the air in Frankfurt is lower than whats expected for the system to be operating in, therefore calculations will be based on a relative humidity of 85 %.

4.2 System Performance During Heating Mode

In this section, the results of the modelling the system during "Heating Mode" will be presented. The model was run at ambient temperatures of 7.5 °C, 2.5 °C, −2.5 °C and −7.5 °C from which the performances of the heat pump can be seen in tab. 4.1. Here it can be seen that heating capacity ranges from 108.1 kW at 7.5 °C to 101.2 kW at −7.5 °C. As the ambient temperature is reduced, both the refrigerant mass flow and the compressor power is reduced. The COP can be assumed constant as the temperature varies, this could be a result of the condensation temperature. As the condensation temperature is lowered, the heat of vaporization of the refrigerant increases. Additionally, since mass flow is reduced, it directly affects the heating capacity, however this also requires less compressor power. The interaction between these parameters thus results in a constant COP.

Results for the Heat Pump System with an SY380-4 Compressor						
T_{amb} [°C]	$\dot{Q}_{cond}$ [kW]	$\dot{m}_{ref}$ [kg/s]	P_{Comp} [kW]	T_{cond} [°C]	T_{evap} [°C]	COP
7.5	108.1	0.53	15.96	26.81	4.863	6.77
2.5	106	0.52	15.62	25.72	4	6.78
-2.5	103.6	0.50	15.25	24.57	3.1	6.79
-7.5	101.2	0.49	14.89	23.42	2.3	6.79

Table 4.1. Model results from the heat pump system.

The results of temperature and relative humidity as the air is processed through the AHU can be seen tab. 4.2. Here it can be seen that with an ambient temperature of 7.5 °C and a relative humidity of 85 %, the heat exchanger can almost provide the necessary heat recovery alone. As a result, the supply air is heated to 35 °C through the heating coil which is 12 °C above the factory temperature. At the coldest ambient conditions of −7.5 °C the heat exchanger heats the air up to 16.9 °C. Here, the heating coil further heats the supply air up to 30.3 °C with a relative humidity of 37.8 %, which is 7.3 °C above the factory temperature.

Results for the Air Handling Unit				
T_{amb} [°C]	RH_{amb} [%]	$T_{after,he}$ [°C]	T_{supply} [°C]	RH_{supply} [%]
7.5	85	19.9	35	35
2.5	85	18.9	33.45	36
-2.5	85	17.9	31.87	37
-7.5	85	16.9	30.3	37.8

Table 4.2. Model results of the AHU.

The reason for the high supply air temperatures of 30.3 °C to 35 °C is a consequence of the SY380-4 compressor being oversized for heating. A solution for reducing the heating capacity could be to increase the condensing and evaporating temperature difference. This would however result in a lower COP thereby make the system inefficient.

The amount of excess heat supplied by the system, as a function of the ambient temperature can be seen in fig. 4.3. Here the excess heating is defined as the amount energy used by the system to heat the air above 23 °C. As it can be in fig. 4.3, even at ambient conditions of −10 °C the system supplies approximately 50 kW excess heat.

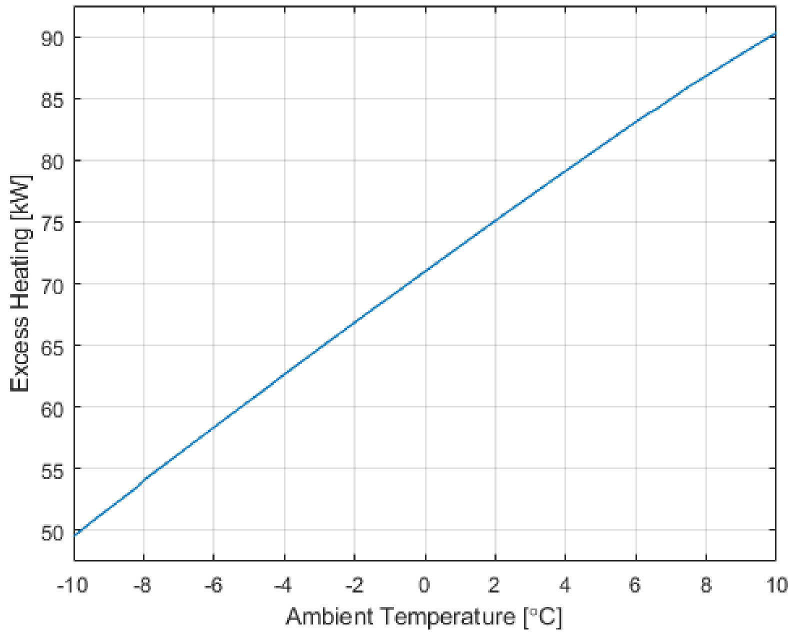

Figure 4.3. Excess heat supplied by the heat pump system at different ambient temperatures.

The results of the cooling water inlet temperatures and power consumption of the cooling tower can be seen in tab. 4.3. Here it can be seen that inlet temperature of the cooling water ranges from 12.05 °C at ambient temperatures of −7.5 °C to 15 °C at temperatures of 7.5 °C. Additionally it can be seen power consumption of the cooling tower almost remains constant.

Results for the Cooling Tower		
T_{amb} [°C]	$T_{CW,in}$ [°C]	P_{CT} [kW]
7.5	15	13.2
2.5	14.05	13.22
-2.5	13.05	13.24
-7.5	12.05	13.26

Table 4.3. Model results for the cooling tower.

In order to gain a wider perspective of the system performance during "Heating Mode", the COP is plotted as a function of the ambient temperature as seen in fig. 4.4 on the facing page.

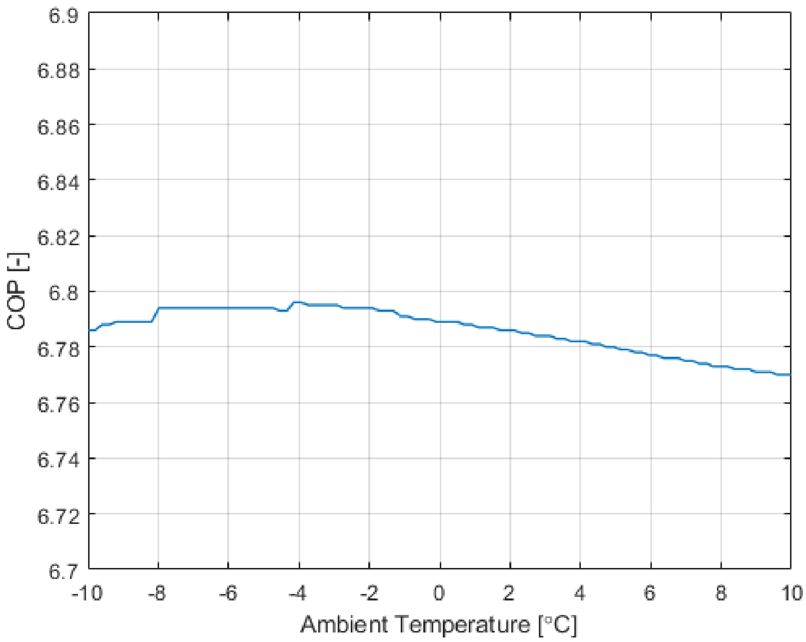

Figure 4.4. COP as a function of the ambient temperature

Here it can be seen that the system COP almost remains constant as the temperature is varied from $-10\,°C$ to $10\,°C$. Furthermore, small spikes can be seen in the graph which could be a result of the none-linear system of equation made in EES.

4.3 System Performance During Cooling Mode

The results from the model during "Cooling Mode" will be presented in this section. The performance of the heat pump system during conditions of 27.5 °C and 32.5 °C with a relative humidity of 85 % can be seen in tab. 4.4. Here, it can be seen that with an ambient temperature of 27.5 °C and a relative humidity of 85 %, the heat pump system's cooling capacity is 101.7 kW. The power consumption of the compressor, P_{Comp} is 18.78 kW which results in a COP of 5.41.

Results for the Heat Pump System with an SY380-4 Compressor						
T_{amb} [°C]	$\dot{Q}_{evap}$ [kW]	$\dot{m}_{ref}$ [kg/s]	P_{Comp} [kW]	T_{cond} [°C]	T_{evap} [°C]	COP
27.5	101.7	0.64	18.78	34.43	10.61	5.41
32.5	109	0.7	20.25	37.91	13.2	5.38

Table 4.4. Model results from the heat pump system.

By increasing the ambient temperature to 32.5 °C, the system's cooling capacity increases to 109 kW. As the ambient temperature rises, it affects both the condensing and evaporation temperature, from which the mass flow of refrigerant and compressor power increases. The mass flow increases from 0.64 kg/s to 0.7 kg/s and the compressor power increases from 18.78 kW to 20.25 kW. Based on this, the COP reduces to 5.38 while operating at ambient temperature of 32.5 °C.

The results of processing the air through the AHU can be seen in tab. 4.5. The air is firstly cooled through a double cross flow heat exchanger utilizing the 23 °C exhaust air from the factory. For an ambient temperature of 27.5 °C, the temperature after the heat exchanger, $T_{after,he}$ is 23.9 °C. As the ambient temperature increases to 32.5 °C, the temperature after the heat exchanger increases to 24.9 °C.

Results for the Air Handling Unit				
T_{amb} [°C]	RH_{amb} [%]	$T_{after,he}$ [°C]	T_{supply} [°C]	RH_{supply} [%]
27.5	85	23.9	20.57	73
32.5	85	24.9	20.91	76

Table 4.5. Model results of the AHU.

During ambient temperatures of 27.5 °C, the air after the heat exchanger will be cooled from 23.9 °C to 20.57 °C over the cooling coil and reach a relative humidity of 73 %. As the ambient temperature increases to 32.5 °C, the air will be cooled down from 24.9 °C to 20.91 °C and reach a relative humidity of 76 %.

The results for the cooling coil and cooling tower can be seen in tab. 4.6 on the next page. Here it is seen that while operating at 27.5 °C, the latent heat, $\dot{Q}_{lat}$ of the coil is 40.68 kW and the sensible heat, $\dot{Q}_{sensi}$ is 61.02 kW. At an operating temperature of 32.5 °C, the latent heat increase to 43.61 kW and the sensible heat to 65.41 kW. As the temperature increases from 27.5 °C to 32.5 °C amount of water condensed over the cooling coil increases from 30.71 g/s to 32 g/s. It can be seen that the cooling tower can provide cooling water of 22 °C, and uses 12.75 kW while operating at 27.5 °C. During operation at 32.5 °C, the cooling water supply temperature is 25.07 °C and uses 12.54 kW.

Results for the Cooling Coil and Cooling Tower					
T_{amb} [°C]	$\dot{Q}_{lat}$ [kW]	$\dot{Q}_{sensi}$ [kW]	$\dot{m}_{cond}$ [g/s]	$T_{CW,in}$ [°C]	P_{CT} [kW]
27.5	40.68	61.02	30.71	22	12.75
32.5	43.61	65.41	32	25.07	12.54

Table 4.6. Model results for the cooling coil and cooling tower.

In order to gain a wider perspective of the system performance during "Cooling Mode", the COP was plotted as a function of the ambient temperature.

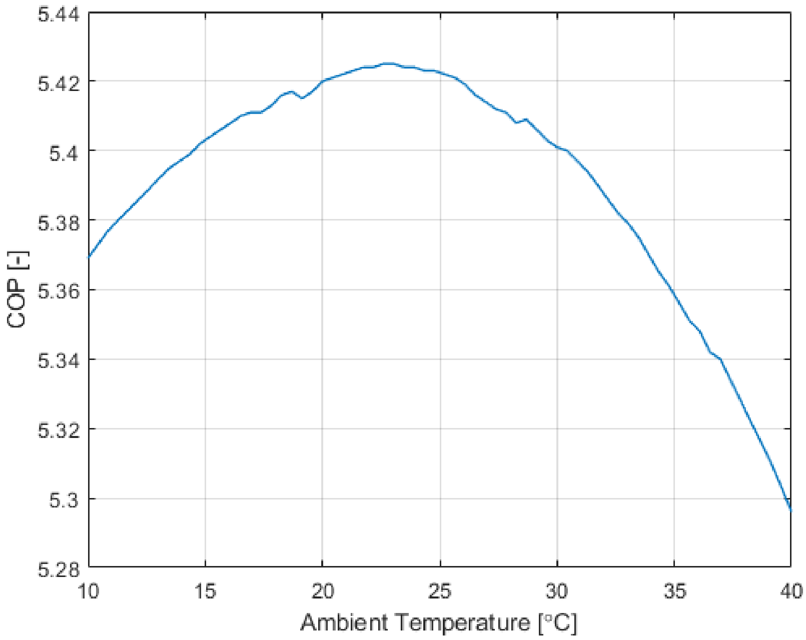

Figure 4.5. COP as a function of the ambient temperature.

As seen in fig. 4.5, the system achieves the highest performance at around 22.5 °C. As the temperature further increases from this point, the performance declines. It should be noted that the change in performance is minor as it can be seen from the range of the y-axis.

Economical Analysis of the Heat Pump System

5

The economical incentive for implementing the heat pump system, is to replace low COP rooftop chillers and gas furnaces, from which both the energy consumption and carbon emissions are reduced. In this chapter the economical aspects of implementing the systems described in chap. 2 on page 3 will be presented. The economical analysis will estimate the capital and operational cost of both the single cycle system and the dual cycle system. Based on the results from the model in chap. 4 on page 31 and the acquired component prices from Danfoss, the CAPEX and OPEX will be estimated. Lastly, the repayment period for implementing the heat pump system compared to a chiller system will be analyzed.

5.1 System Design Considerations

An important aspect to consider during the design phase of the heat pump system, is the component sizes. Generally, it is desired to use larger components since pressure losses are reduced. This reduces the overall power consumption of the compressor and circulation pumps which reduces the OPEX. There is however limitations in terms of the component size since some applications are limited to a certain amount of space available. This could for instance be the space within the AHU where the heat exchangers and compressors are to be installed. Furthermore, increased component sizes directly affects the CAPEX, therefore it is necessary to find a compromise between performance and the price.

In fig. 5.1 on the next page, the price of the H118-E plate heat exchanger as function of the number of plates can be seen. Here it can be seen that there is a linear relation between the price and number of plates. The price ranges from 9,165 DKK for 70 plates to 14,043 DKK for 120 plates. Based on calculations provided by Danfoss, it was suggested that two H118-E heat exchangers with 100 plates were used for the single cycle system. For the dual cycle system four H118-E heat exchangers with 70 plates were suggested. Based on the prices seen in fig. 5.1 on the following page the heat exchangers for the single cycle will cost 24,182 DKK. The cost of the heat exchangers for the dual cycle will be 36,660 DKK. The single cycle system therefore costs 12,478 DKK less that the dual cycle system.

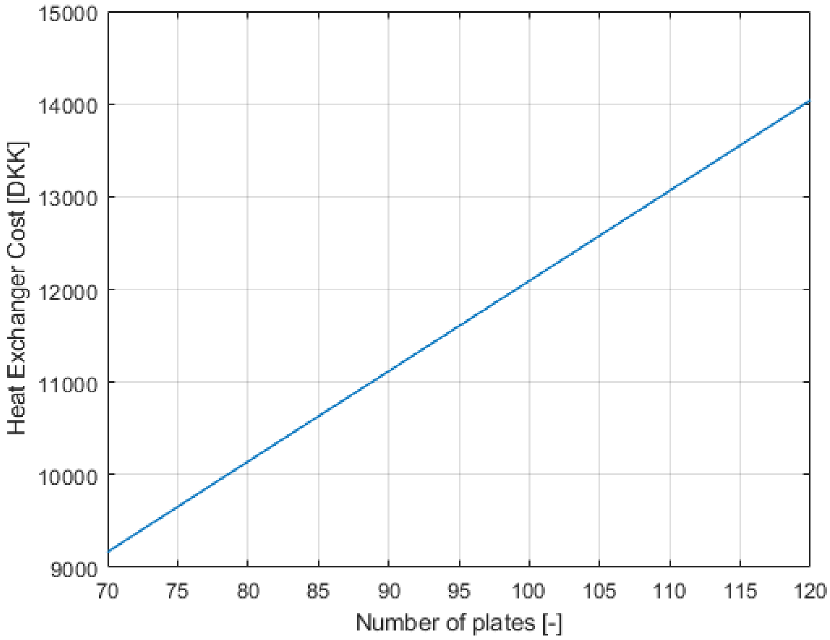

Figure 5.1. H118-E plate heat exchanger price as a function of the number of plates.

In addition to the prices of the heat exchangers, the pressure losses of the two systems were also provided by Danfoss. In tab. 5.1 the pressure losses over a condenser and evaporator during "Cooling Mode" can be seen. The calculations for the single cycle is based on a heat exchanger with 100 plates and the dual cycle is based on two heat exchangers in series with 60 plates. In tab. 5.1, $DP_{cond,ref}$ is the differential pressure over the refrigerant side and $DP_{cond,wat}$ is for the water side of the condenser.

H118-E	$DP_{cond,ref}$ [bar]	$DP_{cond,wat}$ [bar]	$DP_{evap,ref}$ [bar]	$DP_{evap,wat}$ [bar]
Single Cycle	0.74	0.129	2.44	0.092
Dual Cycle	0.95	0.522	3.48	0.528

Table 5.1. Differential pressures over the condenser and evaporator

It can be seen that the single cycle overall has a lower pressure drop over the condenser and evaporator compared to the dual cycle system. As for the evaporator's water side, the pressure loss is almost 0.5 bar less for the single cycle system. To demonstrate the effect of a 0.5 bar difference during operation over a year, a rough estimate will be made. For the circulation pump used in the system, the power consumption as a function of the pressure drop can be seen in tab. 5.2.

Circulation Pump Performance									
DP [bar]	0.5	0.75	1	1.25	1.5	1.75	2	2.25	2.50
Power [kW]	0.464	0.606	0.76	0.922	1.092	1.269	1.453	1.643	1.838

Table 5.2. Differential Pressures over the Condenser and Evaporator

Based on the results from sec. 4.1 on page 31 it was found that the annular operating hours was 4,779 for a system implemented in Frankfurt. Assuming an average electricity of price 2 DKK/kWh, based on the average price estimate by Norlys [21]. Considering that two systems operate, one with 1 bar pressure loss and another with 0.5 bar. For a system with 1 bar pressure loss the annual operation costs will be 7,264 DKK/year. By reducing the pressure loss to 0.5 bar the operation costs reduces to 4,434 DKK/year. As a result, 2,830 DKK/year can be saved yearly which can contribute to reducing the repayment period.

In addition to the examples given in this section, the primary operating mode should also be considered. For instance, if the system operates in "Heating Mode" the majority or the year, the system should be optimized to operate at this condition. This would however compromise the performance of "Cooling Mode", but could provide a cheaper and overall more efficient system.

5.2 Capital Expenditures

In this section, the calculations of the CAPEX for a heat pump system will be presented. The calculations will be made for both the single and the dual cycle system, since a different amount of components are used in both systems. For the calculations, it is assumed that the base cost of an AHU including fans, filters, dampers, heat exchanger and coils is 500,000 DKK. Finally, it is assumed that the cooling tower is already implemented at the factory from which it is not included in the CAPEX.

The components, the quantity of each component and cost can be seen in tab. 5.3 for the single cycle system. The components marked with an "∗" indicates that the exact price could not be acquired, and is therefore based on an estimate.

Component	Quantity	Cost per unit [DKK]	Total cost [DKK]
AHU*	1	500,000	500,000
Circulation pump	2	14,825	29,650
Condenser - 100 plates	1	12,091	12,091
Evaporator - 100 plates	1	12,091	12,091
On/Off Valve	7	3,223	22,561
Expansion Valve*	1	1,500	1,500
Four-way Valve*	1	3,000	3,000
SY380-4 Compressor*	1	80,000	80,000
R407C Refrigerant*	1	15,000	15,000
Total Cost	-	-	**675,893 DKK**

Table 5.3. CAPEX for the single cycle system.

As seen in tab. 5.3 the total CAPEX for the single cycle system is 675,893 DKK. It should be noted that the estimated price for the SY380-4 compressor could differ a lot from the actual price. This is because it was assumed that the compressor had a VLT included, which is an expensive part. The estimations for the expansion valve and the four-way valve was based on conversations with Danfoss. The seven on/off valves are used to redirect the flow as the system changes from

"Heating Mode" to "Cooling Mode". As for the dual cycle system, the components, the quantity of each component and cost can be seen in tab. 5.4

Component	Quantity	Cost per unit [DKK]	Total cost [DKK]
AHU*	1	500,000	500,000
Circulation pump	2	14,825	29,650
Condenser - 70 plates	2	9,165	18,330
Evaporator - 70 plates	2	9,165	18,330
On/Off Valve	7	3,223	22,561
Expansion Valve*	2	1,500	3,000
VLT Compressor*	1	60,000	60,000
Fixed Speed Compressor*	1	20,000	20,000
R407C Refrigerant*	1	15,000	15,000
Total Cost	-	-	**686,871 DKK**

Table 5.4. CAPEX for the dual cycle system.

For the dual cycle system, the total CAPEX is 686,871 DKK which is 10,978 DKK more than the single cycle system. It can be seen that the main reason for the increased cost, is due to double the amount of components are required in the dual system. It is also assumed, that the price of both compressors for a dual cycle is equality to the compressor used in the single cycle.

5.3 Operating Expenditures

In this section, the OPEX for the heat pump system will be presented. The OPEX will be based on the results from the model in chap. 4 on page 31, where the power consumption was found at different operation conditions throughout the year. Since the model is based on a single cycle heat pump system, the OPEX for a dual cycle system can not be determined. As in the sec. 5.1 on page 39, electricity price is assumed to be 2 DKK/kWh.

Since the power consumption of the system was calculated for different temperatures, and also the amount of hours at each temperature, the yearly consumption can now be found. In tab. 5.5 the yearly consumption for operation in "Cooling Mode" can be seen. By operating in "Cooling Mode" for a total of 256 hours the total power consumption is 8,114 kWh.

Component & Temperature	Power [kW]	Operating hours	[kWh]
Compressor (27.5 °C)	18.78	222	4,169.16
Cooling tower (27.5 °C)	12.75	222	2,830.50
Compressor (32.5 °C)	20.25	34	688.50
Cooling tower (32.5 °C)	12.54	34	426.36
Total	-	256	**8,114.52**

Table 5.5. The yearly power consumption and hours for cooling.

The yearly power consumption for operating the system in "Heating Mode" can be seen in tab. 5.6. Here it can be seen that by operating in "Heating Mode" for a total of 4,523 hours 130,765 kWh are consumed over the year.

Component & Temperature	Power [kW]	Operating hours	[kWh]
Compressor (7.5 °C)	15.96	1,731	27,626.76
Cooling tower (7.5 °C)	13.2	1,731	22,849.2
Compressor (2.5 °C)	15.62	2,188	34,176.56
Cooling tower (2.5 °C)	13.22	2,188	28,925.36
Compressor (-2.5 °C)	15.25	543	8,280.75
Cooling tower (-2.5 °C)	13.24	543	7,189.32
Compressor (-7.5 °C)	14.89	61	908.29
Cooling tower (-7.5 °C)	13.26	61	808.86
Total	-	4,523	**130,765.1**

Table 5.6. The yearly power consumption and hours for heating.

The yearly energy consumption for the cooling tower and the compressor has now been determined based on the modelling results. However, additional components such as the fans and circulation pumps should also be considered. Based on data from NB-ventilation the system uses a total of four fans, two 7.5 kW for the supply air and two 5.5 kW for the exhaust air. Assuming these only operate the 4,779 hours during heating and cooling mode, an additional 124,254 kWh will be consumed yearly. For the circulation pump, it is assumed, based on tab. 5.1 on page 40 and 5.2 on page 40 that the pressure drop of the single cycle is 0.5 bar from which the consumption is 0.464 kW. This will result in a yearly power consumption of 2,217 kWh. The individual fractions of the yearly energy consumption for the system can be seen as a pie chart in fig. 5.2.

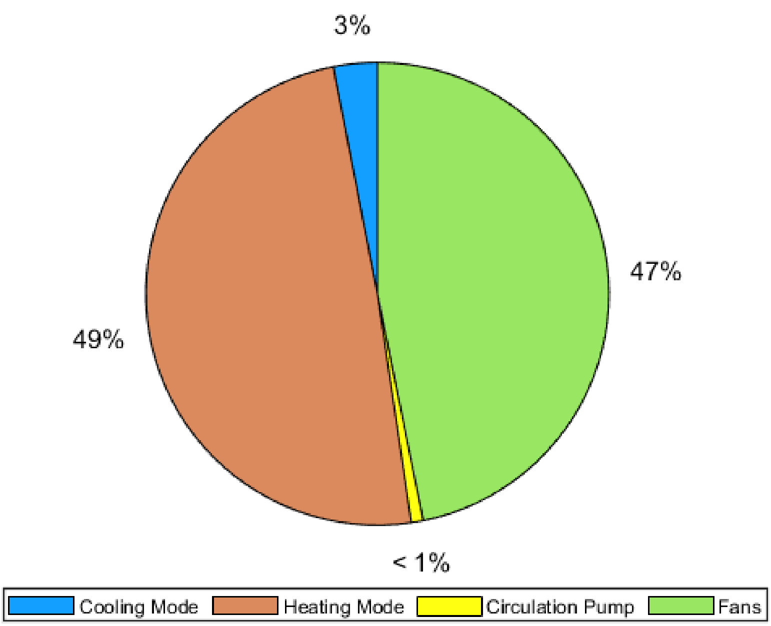

Figure 5.2. Pie chart of the overall power consumption.

As illustrated in the pie chart, the components which makes up for the majority of the power consumption are the fans and the heat pump system during "Heating Mode". Operating in "Heating Mode" makes up for 49 % of total consumption, while the fans makes up for 47 %. As for the operation of "Cooling Mode", it only makes up for 3 % of the total consumption since it only operates 256 hours per year. By running a circulation pump with a 0.5 bar differential pressure it only makes up for $< 1\,\%$. The total yearly power consumption of the system is 265,348 kWh, which makes the OPEX 530,696 DKK.

5.4 Repayment Period

An incentive for implementing the heat pump system, is to replace the old rooftop chiller systems which has a COP of approximately 2 to 3. As it was found from the model results, the heat pump system has a COP ranging from 5.38 to 6.79. This makes the heat pump two to three times more efficient, which could result in a short repayment period. The COP of a vapor compression cycle can be calculated by eq. 5.1 for heating and by eq. 5.2 for cooling. Here it can be seen that the COP indicates the ratio of a systems cooling or heating capacity, in regards to the work supplied. Based on the modelling results, an average cooling and heating capacity was around 105 kW for the heat pump system.

$$COP_{HP} = \frac{\dot{Q}_{cond}}{\dot{P}_{Comp}} \tag{5.1}$$

$$COP_{R} = \frac{\dot{Q}_{evap}}{\dot{P}_{Comp}} \tag{5.2}$$

In order to determine the difference in the work required for a system with a lower COP, eq. 5.1 and 5.2 will be applied. By assuming that $\dot{Q}_{cond}$ and $\dot{Q}_{evap}$ is 105 kW and by varying the COP from 2 to 7, the work can be determined. The results of the required work as a function of the COP can be seen in fig. 5.3.

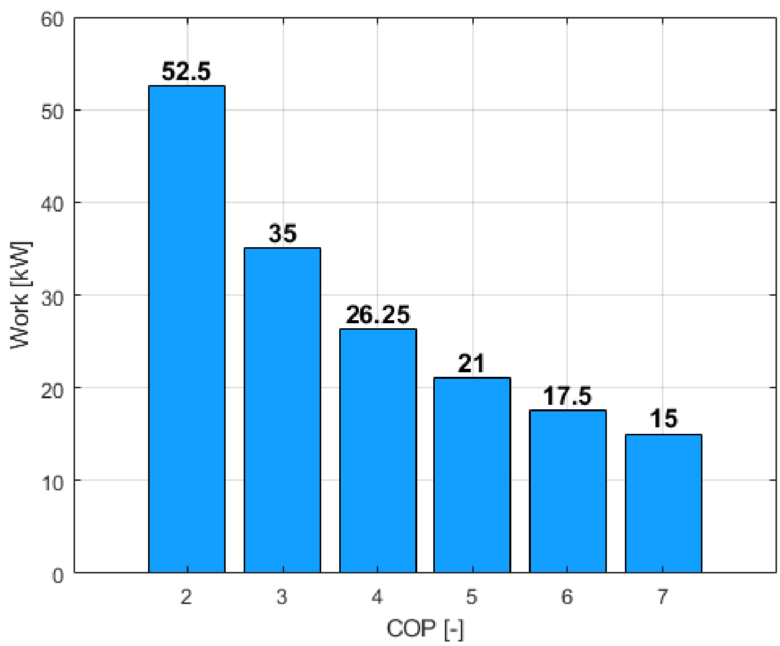

Figure 5.3. Required system work as the COP increases.

Based on the data in fig. 5.3, a COP of 2 will be used as a reference for determining the repayment period. Multiplying the work by the yearly operating hours which is 4,779 and further multiplying with the electricity price of 2 DKK/kWh the yearly price can be determined.

By calculating the annual costs of systems with a COP ranging from 3 to 7 and subtracting it from the system with a COP of 2 the yearly savings can be found as seen in fig. 5.4.

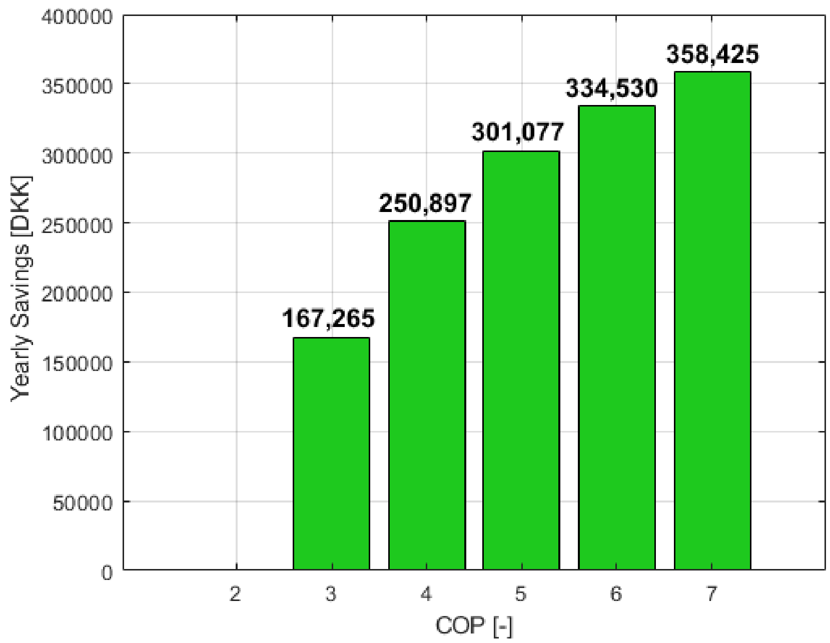

Figure 5.4. Yearly savings relative to a rooftop chiller with a COP of 2 as the new system COP increases.

Finally, the repayment period of the heat pump system can be determined based on the CAPEX calculated in sec. 5.2 on page 41. Here the OPEX for a single cycle system was calculated to be 675,893 DKK, from which the repayment periods can be found as seen in fig. 5.5.

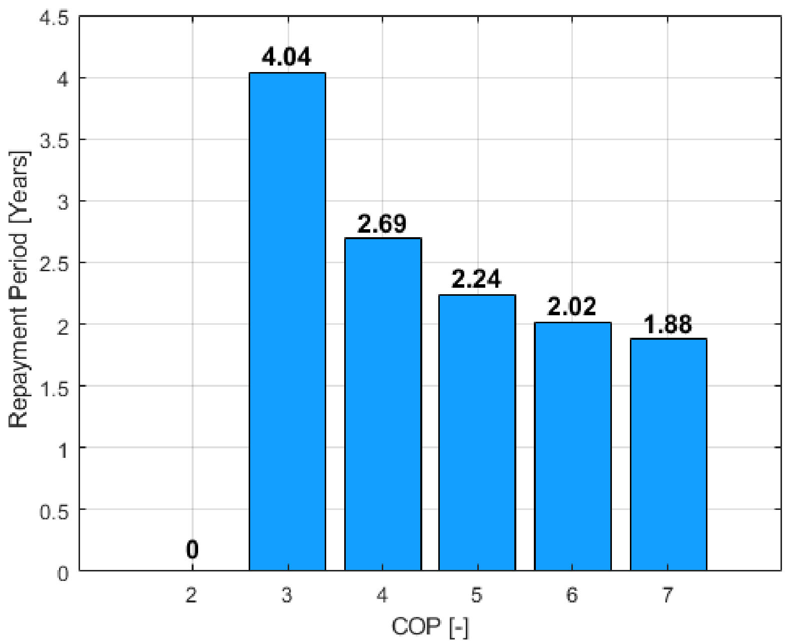

Figure 5.5. Repayment periods relative to a rooftop chiller system with a COP of 2.

It can be seen that by improving the COP from 3 to 4 it lowers the repayment period by almost 1.5 year. However, further improving the COP from 4 to 7 has a minor effect on the repayment period, which is lower by less than one year. It should be noted that the repayment period found still provides a strong financial incentive to invest in the heat pump system. Since the calculations are based on a system with a COP of 2, it provides good result in terms of the repayment periods. Therefore it should be analyzed how the repayment periods are affected by using a system with a COP of 3 as a baseline for the calculations. The repayment periods achieved by replacing a chiller system with a COP of 3 with a new system that has a COP of either 4, 5, 5 and 7 can be seen in fig. 5.6.

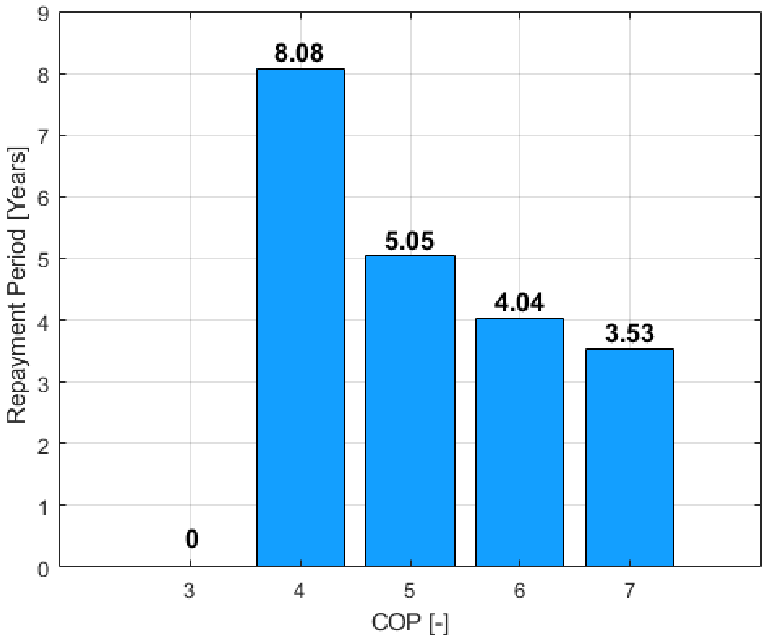

Figure 5.6. Repayment periods relative to a rooftop chiller system with a COP of 3.

It can be seen that this doubles the repayment periods of the heat pump system. However, considering that heat pump system has a COP of 5.38 to 6.79 according the model, it can be estimated that the repayment period with be approximately 4 to 5 years. As for the longer repayment period, additional expenditures should be considered in the economical analysis. In order to account for inflation, maintenance or replacement of old components throughout the system lifetime, the NPV (Net Present Value) will be calculated. The NPV can determine the present value of an investment by taking into account for future incomes and expenditures. The present value for a given amount of money in the future, can be described by eq. 5.3.

$$PV = CM_n \cdot \frac{1}{(1+r)^n} \tag{5.3}$$

Here, PV (Present Value) is the present value n amount of years in the future and CM_n is the income subtracted from the expenses that year. The yearly inflation rate will be described by r

which is assumed to be 0.03. In order to show the effect of inflation on the yearly savings found in fig. 5.4 on page 46, a short example will be presented. By implementing the new system with a COP of 5, the yearly savings was found to be 301,077 DKK/year. Based on eq. 5.3 on the preceding page the yearly savings 5 years from now reduces from 301,077 DKK/year to 259,711 DKK/year assuming a yearly inflation of 3 %. In order to determine a NPV over the lifetime, the assumed expenditures and their costs also has to be defined as seen in tab. 5.7.

Expenditure	**Occurrence**	**Price** [DKK]
Maintenance	every year	10,000
Change of filters	after 5 years	10,000
Change of refrigerant	after 10 years	15,000
Change of fans	after 10 years	24,000

Table 5.7. Assumed expenses over a system lifetime.

Based on the occurrence of the expenditures, it can be seen that the contribution margin CM_n will vary accordingly. For example the CM_n after 10 years will be calculated as seen in eq. 5.4 based on the expenditures in tab. 5.7.

$$CM_{10} = (Income - 10,000 - 15,000 - 24,000) \tag{5.4}$$

By assuming a lifetime of 10 years, the contribution margin has to be calculated and applied in eq. 5.3 on the preceding page for each year. In addition to this the yearly income will be calculated based on a payback time of 8, 5 and 4 years. As a result the initial investment cost of 675,893 DKK, the yearly incomes for a repayment period of 8, 5, and 4 years will be 84,487 DKK, 135,180 DKK and 168,970 DKK as seen in fig. 5.7.

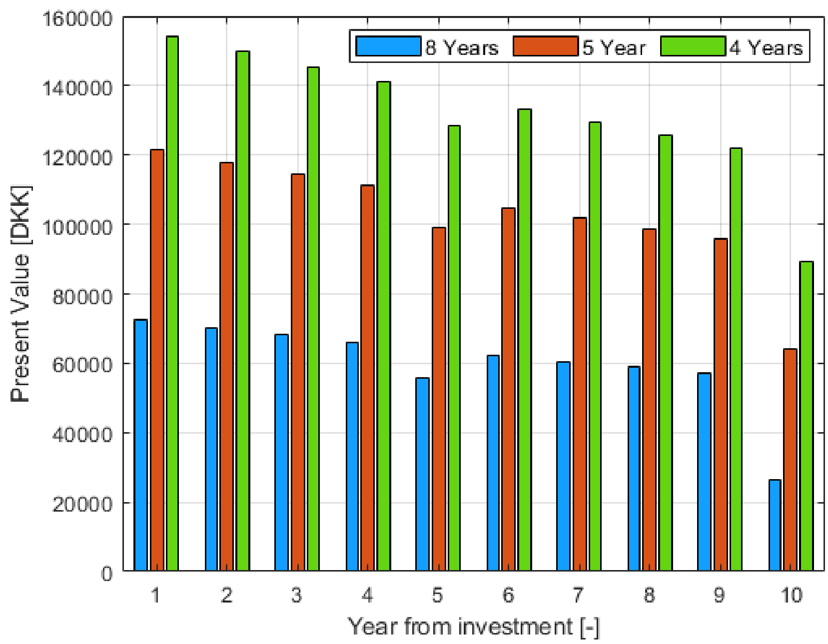

Figure 5.7. Present values including expenditures for a system lifetime of 10 years.

By summing up the PVs and subtracting the initial investment cost, the NPV of the system based on a repayment period of 8, 5 and 4 years can be determined. As seen in fig. 5.8 a system with a repayment period of 8 years will not provide sufficient income to cover the expenses and inflation. However, utilizing a system which has a repayment period of 4 or 5 years will result in a return of investment of 354,000 DKK or 642,507 DKK over a 10 year period.

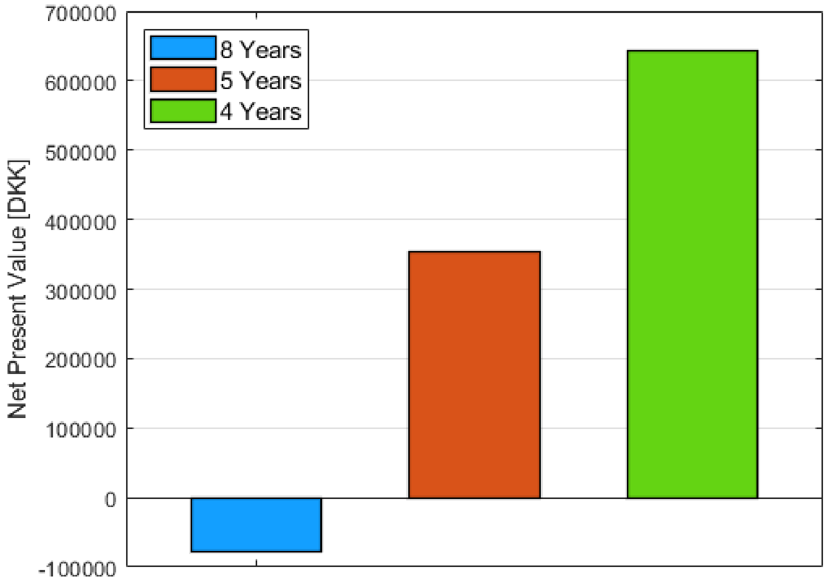

Figure 5.8. Net Present values over a lifetime of 10 years.

Based on the economical analysis throughout this system it can be concluded that the system should have a COP of at least 5, from which the return of investment becomes positive. Generally, this indicates the importance of developing a specific compressor for this system since it directly affects the business potential.

Discussion 6

In this chapter a discussion of the different aspects, considerations and results in regards to the heat pump system will be presented.

6.1 System Designs and Components

In this study, two systems configurations has been presented in sec. 2.3 on page 7, a single cycle and a dual cycle which both has their advantages and disadvantages. By implementing a single cycle the amount of heat exchangers and space required are reduced, however the operational reliability is affected. Assuming that one of the compressors within the hybrid manifold break downs the whole system will stop operating. As for the dual cycle, if one of the compressors breaks down, the other cycle can still operate at half capacity. Furthermore, the issues of coupling compressors in parallel through the hybrid manifold should be considered. Generally, it is important to monitor the oil level and ensure that the lubrication oil is being distributed equally between the two compressors during operation. The hybrid manifold system was chosen since no compressors with a VLT was available on the market which could provide the desired capacity and used R407C. However, Danfoss is developing a new compressor series called Turbocor which has a VLT and capacities greater than 140 kW [22]. Additionally, the Turbocor compressor is oil free and uses HFO refrigerant such as R1234ze. By utilizing a Turbocor compressor for the heat pump system, the hybrid manifold could be replaced by a simplere and reliable system. However, since no data of the Turbocor performance is available, the affect on the COP is unknown. As for the performance difference between the single cycle of dual cycle, it is unknown since no data sheets for the hybrid manifold compressors could be found. However, it is assumed that the single cycle would perform better since the compressors are directly coupled to each other. As a result of this, it assumed that the heating and cooling effects could be regulated more precisely compared to the two compressors in the dual cycle.

Throughout this study, the SY380-4 compressor was used since it had enough capacity to cover the cooling load in the summer. As a result of the compressor accounting for the cooling requirements during summer, the heating capacity during winter was exaggerated. At ambient temperatures of $-10\,°C$ the compressor provided 50 kW more than required which resulted in a supply air temperatures of $30.3\,°C$. Based on the weather data from Frankfurt, in a year only 256 hours out of 4779 hours required cooling. Therefore the smaller VTZ215-G compressor which was originally chosen for the system could have been a good fit for heating, however this would compromise the cooling performance during summer. Furthermore it is important to consider that the compressor performance is directly affected by the temperature lift between the condenser and evaporator. In "Heating Mode", the system had a low temperature lift of around 21 °C which resulted in a high COP. However, in reality the compressor might not be able to achieve such a performance under these conditions. In the SY380-4 data sheet, the minimum condensing temperature stated is 30 °C, however in "Heating Mode" a temperatures of 23.4 °C was reached. This could also an indicate that the compressor might not operate as well under these conditions in reality.

As for the heat exchangers, the H118-E series from Danfoss was chosen, since these are optimized for the refrigerant R407C. Additional the size could be selected in the based on the amount of plates desired, which was 70 or 100 in the systems. Generally it is desired by Danfoss to achieve a low pressure losses over components such as valves and heat exchangers. The main consideration for the heat exchangers is the compromise between a low pressure loss and the size. As two heat exchangers with 70 plates in series are used for the dual cycle, the pressure loss in the water-side was around 0.4 bar compared with the single cycle. For the refrigerant side in a dual cycle, the pressure loss over the evaporator was 1 bar greater compared with the single cycle. Therefore it should be considered to increase the number of plates used for the heat exchangers in the dual cycle system to reduce the pumping power.

The heating and cooling coil provided by TT-Coil uses a brine consisting of water and 30% EG, to prevent frost damage of the coils. However the consequence of using the mixture compared just pure water lowers the capacity of the coil. By implementing a safety system in AHU such that cold air would never reach the coils during e.g. damper malfunctions, water could be used instead. Based on this it could be possible to apply smaller and more efficient heating and cooling coils.

6.2 Model Assumptions and Consideration

The model was based on the assumption that the heat transfer in the evaporator and the condenser was equal to the cooling or heating provided in the heating coil. For a real system this would not be the case since temperature losses to the surroundings occur. As a result, the heating and cooling capacity of the compressor should be increased slightly for a real system to account for this. Furthermore, it was also assumed that the EG/Water in the model was just pure water. This could have caused some insecurities in regards to the temperatures of the EG/water flow since the thermophysical properties varies. An assumption was also that the inlet quality of the refrigerant in the evaporator was 0.25 and the outlet quality was 1 with a 3 K. Based on conversation with Danfoss the inlet quality could range from 0.2 to 0.3 which directly affects the capacity of the evaporator.

An important aspect in regards to the modelling, is the bi-quadratic interpolation method used for both the compressor and the heat exchangers. By utilizing high order polynomials for interpolation it can result in a major uncertainty while extrapolating outside the of the known data points. As for the condensation temperature, the lowest data point is at 30 °C based on the data sheet. However during modelling of "Heating Mode" the condensation temperature ranged from 23.42 °C to 26.81 °C, therefore the results found may not have been reliable.

In order to account for the dehumidification of the air, it was assumed that 30% of the inlet moist content was removed over the cooling coil. For a real system this would not have been the case, since the dehumidification process is controlled by a moisture sensor. In addition to this, the method used to control the compressor through the outlet temperature of the flows in the condenser and evaporator is not ideal. For a better performance and control of the system, the model should have included the implementation of a VLT. This could for instance have reduced the capacity during "Heating Mode" where too much heating has provided by the system.

6.3 Future Choice of Refrigerant

The choice of the refrigerant is one of the most important aspects to consider for the heat pump system. The refrigerant can directly affect the compressor performance, price but also the system lifetime. In this study R407C was used, this is however an old refrigerant which is being phased out. The reason for using R407C is that the old compressors which Danfoss had available uses it, based on this it would be a cheap solution for testing the prove of concept. According to Danfoss the future replacements for R407C are low GWP refrigerant blends which was shown in fig. 2.8 on page 9. It should be strongly considered to design a system which uses low GWP blends or HFO's since forced regulations could be imposed as a part of the future green transition. The result of having to replace the refrigerant in an existing system could be a lower performance, since the characteristics in terms of density, heat of vaporization, operating temperature and pressure differs. In some cases the new refrigerant might not be applicable for the compressor or heat exchangers from which a whole new system must be implemented. An other incentive for using low GWP refrigerants are imposed taxes and limitations of the refrigerant charge in a system with high GWP refrigerant. Therefore, in a relation to the system as a future investment this must be carefully considered.

6.4 Economical Aspects

For the economical calculations it was assumed that that the electricity price is 2 DKK/kWh based on Norlys [21]. However the development of the future electricity prices should be considered as more renewable energy sources such as wind- and solar power are implemented. Energinet has published a paper which studies how the electricity price is affected as the amount of wind- and solar power increases. It should be noted that these are based on some optimistic and unrealistic scenarios, however it can provide a good insight for future tendencies. The future price estimates from Energinet over the 8,760 hours of year can be seen in fig. 6.1. [23]

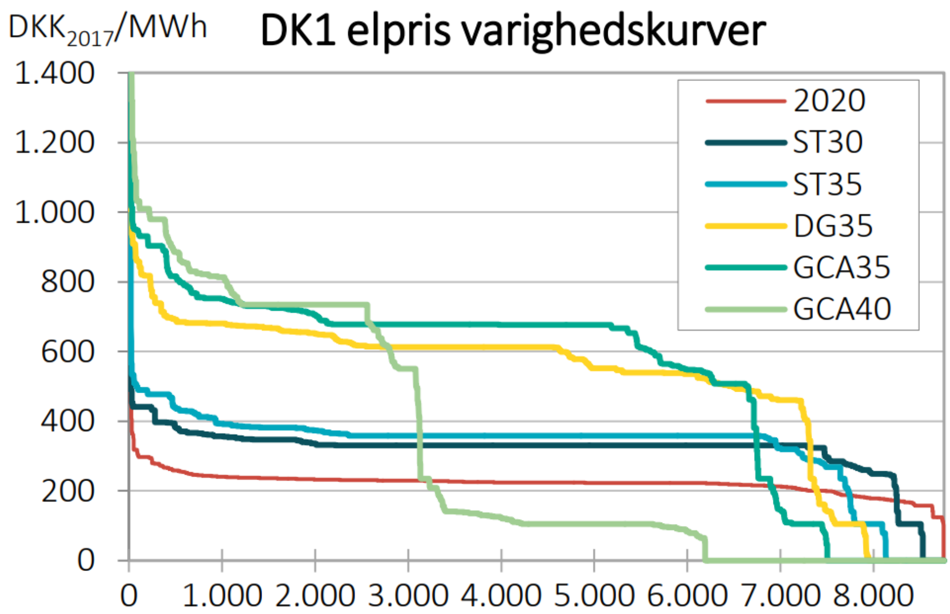

Figure 6.1. Estimated future electricity price based on future renewable scenarios. ([23] Page 7)

The fluctuation in electricity price is result of the fluctuating energy production from wind- and solar power in addition to the supply and demand. This leads do high prices during high demand and low production and low prices during high production and low demand. As a result, the electricity price can become negative from which you get paid for using electricity. Applying such a scenario to the heat pump system could further improve the business potential as this would improve the repayment period. Since a purpose of the system also is to replace gas furnaces used for heating, the future carbon taxes could also provide a financial incentive for companies replace their old systems. For existing systems in the U.S with gas furnaces it can be hard to compete with the low natural gas prices of 5 to 7 Øre/kWh according to Danfoss. Therefore future carbon taxes could also boost the incentive for replacing old systems.

In the study it was found that the a realistic repayment period of the system would be around 4 to 5 years. However, this is strongly dependent on the performance in terms of the COP. Therefore it is important for Danfoss to develop a state-the-of-the-art Turbocor compressor, which can operate under a low temperature lift and provide high heating and cooling capacities. As it was found the NPV over 10 years for a system with a repayment period of 4 and 5 years was 354,000 DKK and 642,000 DKK. The NPV accounted for simple expenditures, inflation and maintenance, so even if some additional expenditures was not accounted for the NPV would most likely still be positive. Also the system lifetime was assumed to be 10 years, however the lifetime of an AHU could possible be 15 years or longer based on experience from NB-ventilation. Generally, from the results found, the heat pump system would make an attractive investment, however this would strongly depend on performance of a real life system.

6.5 Results

Generally, the results provided by the model seems to be reliable taking into consideration the assumptions and uncertainties associated with it. However, in order to validate the modelling results the prototype system should be build of the components found through this study. Based on this, experiments and measurements should be conduced from which the performance could be directly compared. As for the economical results, these also seem reliable, specially the CAPEX found since it is based on real prices of the components. As for the NPV over 10 years, it could vary from the calculated result as the actual price of the expenditures is unknown. Overall, the results from economical analysis provides good results, which indicates that the heat pump system could have a great business potential.

Conclusion and Future Work 7

In this study, the implementation and modelling of a heat pump system which is coupled between a cooling water network and a ventilation unit has been investigated. This study lays the future groundwork for building and implementing a prototype system, located at a Danfoss factory in Neumünster. The objective was to determine the system performance as a function of the ambient temperature over the year. In addition to this an economical analysis should be made which should determine the CAPEX, OPEX and repayment period of the system.

In order to model the system, real components which are available on the market was firstly selected. Based on this, the compressor chosen was the SY380-4 compressor in combination with two H118-E heat exchangers. The SY380-4 did not have a VLT, however it could provide the desired cooling and heating capacity. Based on analyzed weather data it was found that the system would operate 4779 hours a year, where 256 hours required cooling and the remaining 4,523 hours required heating. From this, it can be concluded that the compressor should be selected based on the primary operation condition. From the model it can be concluded that the system could achieve a COP of 6.7 in "Heating Mode" and a COP of 5.41 in "Cooling Mode" Additional it can be concluded that the SY380-4 compressor was oversized for heating. As a result, the supply air was heated up to 35 °C from which the desired factory temperature was only 23 °C. Based on this it can be concluded that a VLT is a requirement for the chosen compressor in the prototype system. It can be concluded that during "Cooling Mode" the SY380-4 compressor system was a good fit, since it provided supply temperatures of 21 °C.

In terms of the economical analysis, it can be concluded that the system shows a good potential as a future investment. The CAPEX for the system was found to be 657,893 DKK with a yearly OPEX of 265,348 DKK. By achieving a system COP of 5 to 6 the repayment period of the system would be around 4 to 5 years compared to chiller system. Based on the performance of the heat pump system and the economical analysis, it can be concluded that the system has a great potential to replace old rooftop chillers and gas burners. However to ensure this, the prototype should be build from which the performance can be validated.

Future Work

The main objective of this study was to acquire knowledge about the performance and the design of the heat pump system. This should lay the groundwork for building and implementing a future prototype at a Danfoss factory located in Neumünster. The future work would therefore consist of building a prototype with the components chosen throughout this study. In addition to this, experiments and measurements should be conducted such the actual performance can be determined. Furthermore, a model should be made based on the measurements and experiments, which can be used to design future systems for other factories. The prototype system uses the old R407C refrigerant which is being phased out by low GWP HFO-refrigerants in the near future. Therefore, as the concept of this system has proven to work, it should be developed such that HFO's can by utilized as the refrigerant.

Bibliography

[1] U.S. Energy Information Administration. *Energy and the environment explained - Greenhouse gases and the climate*. https://www.eia.gov/energyexplained/energy-and-the-environment/greenhouse-gases-and-the-climate.php. Seen: 08/03-2021.

[2] Rebecca Lindsey. *Climate Change: Atmospheric Carbon Dioxide*. https://www.climate.gov/news-features/understanding-climate/climate-change-atmospheric-carbon-dioxide. Seen: 17/02-2021.

[3] European Commission. *2030 climate and energy framework*. https://ec.europa.eu/clima/policies/strategies/2030_en. Seen: 16/02-2021.

[4] European Commission. *Energy performance of buildings directive*. https://ec.europa.eu/energy/topics/energy-efficiency/energy-efficient-buildings/energy-performance-buildings-directive_en. Seen: 16/03-2021.

[5] Danfoss. *Danfoss targets CO2 neutrality latest by 2030*. https://www.danfoss.com/en/about-danfoss/news/cf/danfoss-targets-co2-neutrality-latest-by-2030/. Seen: 16/03-2021.

[6] Folke Pedersen. *Oplæg til varmepumper i ventilationsanlæg og recirkulerings fortirnsvis til produktionsfabrikker med køling og affugtning*. Seen: 17/03-2021.

[7] Shailendra Kasera, Prof. Shishir Chandra Bhaduri. *Performance of R407C as an Alternate to R22: A Review - RAAR 2016*. Seen: 04/04-2021.

[8] Danfoss. *Refrigerant options now and in the future - Updated February 2020*. https://assets.danfoss.com/documents/157093/AD224586434178en-000803.pdf. Seen: 04/04-2021.

[9] John W. Mitchell, James E. Braun. *Principles of Heating, Ventilation and Air Conditioning in Buildings - chap. 15*. Seen: 04/04-2021.

[10] Mads Pagh Nielsen. *Lecture: Modellering af Termiske Systemer, Autumn 2020 - Real refrigeration cycles, compressors and refrigerants*. Seen: 06/04-2021.

[11] Danfoss. *Ny VTZ Compressor Drive*. https://assets.danfoss.com/documents/95144/AD138186437006da-000101.pdf. Seen: 08/04-2021.

[12] Arkadiusz Guzda, Norbert Szmolke. *Compressors in Heat Pumps - Scientific Figure on ResearchGate*. `https://www.researchgate.net/figure/Simplified-diagram-of-a-reciprocating-compressor1-compressor-suction-area-2-working_fig3_313134829`. Seen: 05/04-2021.

[13] The Workshop Compressor. *The Scroll compressor: quiet and easy.* `http://theworkshopcompressor.com/learn/compressor-types/scroll-compressor/`. Seen: 27/05-2021.

[14] Danfoss. *Inverter scroll compressors - VZH hybrid manifold.* `https://assets.danfoss.com/documents/90367/AB298632269085en-000101.pdf`. Seen: 20/04-2021.

[15] Nellis G. and Klein S. *Heat transfer - Cambridge University Press*, 2009.

[16] Jesús Moreno Quibén. *Experimental and analytical study of two-phase pressure drops during evaporation in horizontal tubes.* `https://www.researchgate.net/publication/37421723_Experimental_and_analytical_study_of_two-phase_pressure_drops_during_evaporation_in_horizontal_tubes`. Seen: 18/04-2021.

[17] Hong Hu, Cheng Xu, Yang Zhao, Krik J. Ziegler J. N. Chung. *Boiling and quenching heat transfer advancement by nanoscale surface modification.* `https://www.nature.com/articles/s41598-017-06050-0`. Seen: 19/04-2021.

[18] Torsten Berning. *Lecture 13 Slideshow - Course: Varmetransmission/heat transfer, Autumn 2018 - Boiling and Condensation*. Seen: 19/04-2021.

[19] James W. Westwater - Department of Chemical Engineering, University of Illinois, Urbana II, U.S.A. . *Gold surfaces for condensation Heat transfer.* `https://link.springer.com/content/pdf/10.1007/BF03216737.pdf`. Seen: 20/04-2021.

[20] Unilab. *Evaporators and condensers: counter-current or co-current arrangement.* `https://www.unilab.eu/articles/technical-articles/thermodynamic-engineering-articles/counter-current-co-current-arrangement/`. Seen: 02/05-2021.

[21] Norlys. *Hvad koster en kWh.* `https://norlys.dk/el/vaerd-at-vide/kwh-kilowatttimer`. Seen: 19/05-2021.

[22] Danfoss. *The Danfoss Turbocor - Portfolio of Oil Free Compressors.* `https://assets.danfoss.com/documents/97592/AD263605305979en-010101.pdf`. Seen: 27/05-2021.

[23] Energinet. *Systemperspektiv 2035.* `https://energinet.dk/systemperspektiv2035`. PDF can be downloaded in the link, Seen: 27/05-2021.

[24] Danfoss. *Inverter Reciprocating Compressors VTZ215-G.* https://assets.danfoss.com/documents/77073/AI157386420255en-000402.pdf. Seen: 05/04-2021.

[25] Danfoss. *Danfoss Scroll Compressors SY380-4.* https://assets.danfoss.com/documents/87565/AI224586434276en-000701.pdf. Seen: 12/04-2021.

Compressor Data sheets

A

The full data sheet for the VTZ215-G compressor can be found at [24].

Danfoss

Datasheet, technical data — **Inverter reciprocating compressors VTZ215-G**

General Characteristics

Model number (on compressor nameplate)	**VTZ215AGNR1A**
Code number for Singlepack*	120B0006
Drawing number	8504018a
Suction and discharge connections	Rotolock
Suction connection	1-3/4 " Rotolock
Discharge connection	1-1/4 " Rotolock
Suction connection with supplied sleeve	1-1/8 " ODF
Discharge connection with supplied sleeve	3/4 " ODF
Oil sight glass	Threaded
Oil equalisation connection	3/8" flare SAE
Oil drain connection	None
LP gauge port	Schrader
IPR valve	30 bar / 8 bar
Cylinders	4
Swept volume	215.44 cm3/rev
Net weight	64 kg
Oil charge	3.9 litre, POE - 160PZ
Maximum system test pressure Low Side / High side	25 bar(g) / 30 bar(g)
Maximum differential test pressure	30 bar
Maximum number of starts per hour	12
Refrigerant charge limit	10 kg
Approved refrigerants	R404A, R507A, R134a, R407C

Dimensions

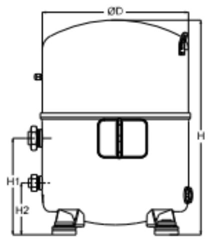

D=352 mm
H=518 mm
H1=233 mm
H2=125 mm
H3=- mm

Electrical Characteristics

Nominal voltage	Frequency converter CD302 required with supply voltage 380-480V/3/50-60Hz
Voltage range	342-528 V supply to frequency converter
Winding resistance (between phases) +/- 7% at 25ºC	0.47 Ω
Rated Load Amps (RLA)	40.8 A
Maximum Must Trip current (MMT)	51 A
Locked Rotor Amps (LRA)	197 A
Motor protection	Motor protection by frequency converter

Terminal box

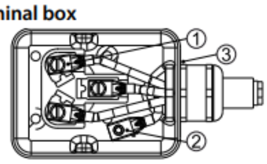

IP54 (with cable gland)
1: Power connection, 3 x 4.8 mm (3/16")
2: Earth M4
3: Hole Ø 33 mm (1.30")

Recommended Installation torques

Oil sight glass	50 Nm
Power connections / Earth connection	3 Nm / 2 Nm
Mounting bolts	50 Nm

Parts shipped with compressor

Mounting kit with grommets, bolts, nuts, sleeves and washers
Suction & Discharge solder sleeves, rotolock nuts and gaskets (shipped with rotolock version only)
Initial oil charge
Installation instructions

Datasheet, performance data **Inverter reciprocating compressors VTZ215-G**

Performance data at 90 Hz, ARI rating conditions **R407C**

Cond. temp. in °C (tc)	Evaporating temperature in °C (to)								
	-17.5	-15	-10	-5	0	5	10	15	

Cooling capacity in W

20	26 374	30 141	38 765	48 981	60 959	-	-	-	-
30	22 772	26 320	34 400	43 936	55 097	68 052	82 971	-	-
40	18 984	22 275	29 738	38 519	48 789	60 718	74 477	90 236	-
45	-	20 190	27 317	35 693	45 490	56 881	70 035	85 123	-
50	-	-	24 848	32 802	42 110	52 944	65 476	79 879	-
55	-	-	-	29 855	38 657	48 919	60 816	74 518	-
60	-	-	-	26 863	35 144	44 821	56 069	69 060	-
65	-	-	-	-	31 586	40 667	51 257	63 532	-

Power input in W

20	10 301	10 932	12 142	13 250	14 218	-	-	-	-
30	10 932	11 705	13 246	14 747	16 171	17 480	18 635	-	-
40	11 379	12 274	14 108	15 965	17 808	19 598	21 296	22 866	-
45	-	12 505	14 471	16 492	18 529	20 546	22 503	24 361	-
50	-	-	14 800	16 975	19 199	21 432	23 637	25 776	-
55	-	-	-	17 425	19 825	22 266	24 710	27 118	-
60	-	-	-	17 849	20 416	23 055	25 729	28 398	-
65	-	-	-	-	20 982	23 810	26 703	29 624	-

Current consumption in A

20	13.23	13.94	15.27	16.56	17.85	-	-	-	-
30	14.02	14.97	16.77	18.49	20.19	21.93	23.76	-	-
40	14.47	15.67	17.96	20.14	22.28	24.42	26.63	28.96	-
45	-	15.89	18.43	20.86	23.22	25.57	27.98	30.49	-
50	-	-	18.81	21.48	24.08	26.65	29.26	31.97	-
55	-	-	-	22.02	24.85	27.65	30.47	33.38	-
60	-	-	-	22.46	25.54	28.57	31.61	34.72	-
65	-	-	-	-	26.13	29.40	32.66	35.98	-

Mass flow in kg/h

20	472	537	681	849	1 042	-	-	-	-
30	441	506	652	820	1 014	1 235	1 488	-	-
40	402	467	613	782	975	1 196	1 448	1 732	-
45	-	444	591	759	952	1 173	1 424	1 707	-
50	-	-	565	733	926	1 146	1 396	1 679	-
55	-	-	-	705	897	1 117	1 366	1 647	-
60	-	-	-	673	865	1 084	1 332	1 612	-
65	-	-	-	-	830	1 047	1 294	1 573	-

Coefficient of performance (C.O.P.)

20	2.56	2.76	3.19	3.70	4.29	-	-	-	-
30	2.08	2.25	2.60	2.98	3.41	3.89	4.45	-	-
40	1.67	1.81	2.11	2.41	2.74	3.10	3.50	3.95	-
45	-	1.61	1.89	2.16	2.46	2.77	3.11	3.49	-
50	-	-	1.68	1.93	2.19	2.47	2.77	3.10	-
55	-	-	-	1.71	1.95	2.20	2.46	2.75	-
60	-	-	-	1.50	1.72	1.94	2.18	2.43	-
65	-	-	-	-	1.51	1.71	1.92	2.14	-

Nominal performance at to = 7.2 °C, tc = 54.4 °C

Cooling capacity	54 462	W
Power input	23 233	W
Current consumption	28.76	A
Mass flow	1 226	kg/h
C.O.P.	2.34	

to: Evaporating temperature at dew point
tc: Condensing temperature at dew point
Rating conditions : Superheat = 11.1 K , Subcooling = 8.3 K

Pressure switch settings

Maximum HP switch setting	29.4	bar(g)
Minimum LP switch setting	0.2	bar(g)
LP pump down setting	1.3	bar(g)

Sound power data

Sound power level	0	dB(A)
With accoustic hood	0	dB(A)

-

FRCC.ED.VTZ215-G.A4.02 / page performance R407C 90 Hz

The full data sheet for the SY380-4 compressor can be found at [25].

Datasheet, technical data — Danfoss scroll compressor, SY380-4

General Characteristics

Model number (on compressor nameplate)		**SY380A4CAE**
Code number for Singlepack*		SY380A4CAI
Code number for Industrial pack**		SY380A4CAM
Drawing number		8556093b
Suction and discharge connections Suction connection Discharge connection		Brazed 2-1/8 " ODF 1-3/8 " ODF
Oil sight glass Oil equalisation connection Oil drain connection LP gauge port IPR valve Reverse rotation protection		Threaded 1/2" flare 1/4" flare Schrader Yes Electronic module
Swept volume Displacement @ Nominal speed	531.2 cm3/rev 92.4 m3/h @ 2900 rpm - 111.6 m3/h @ 3500 rpm	
Net weight Oil charge	158 kg 8.4 litre, POE - 320SZ	
Maximum system test pressure Low Side / High side Maximum differential test pressure	20 bar(g) / 27.9 bar(g) 24 bar	
Maximum number of starts per hour	12	
Refrigerant charge limit	20 kg	
Approved refrigerants	R22, R134a	

Dimensions

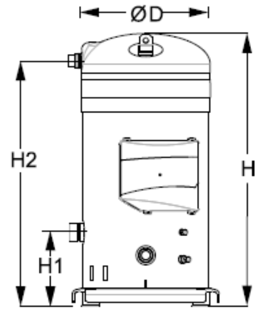

D=344 mm
H=726.9 mm
H1=195.7 mm
H2=654 mm
H3=- mm

Electrical Characteristics

Nominal voltage	380-415V/3/50Hz - 460V/3/60Hz
Voltage range	340-457 V @ 50Hz - 414-506 V @ 60Hz
Winding resistance (between phases) +/- 7% at 25ºC	0.410 Ω
Rated Load Amps (RLA)	56.4 A
Maximum Continuous Current (MCC)	79 A
Locked Rotor Amps (LRA)	300 A
Motor protection	Electronic protection module, 24 V AC

Terminal box

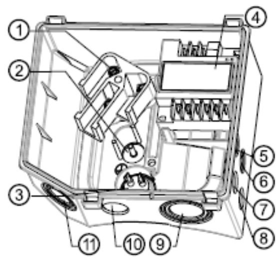

Recommended Installation torques

Oil sight glass	50 Nm
Power connections / Earth connection	3 Nm / 2 Nm
Mounting bolts	40 Nm

Datasheet, performance data **Danfoss scroll compressor. SY380-4**

Performance data at 60 Hz, ARI rating conditions **R407C**

Cond. temp. in °C (tc)	Evaporating temperature in °C (to)								
	-20	-15	-10	-5	0	5	10	15	

Cooling capacity in W

30	45 204	56 744	70 444	86 587	105 455	127 332	152 499	181 240	-
35	42 922	54 086	67 304	82 859	101 033	122 108	146 368	174 095	-
40	40 505	51 250	63 943	78 865	96 300	116 531	139 839	166 508	-
45	37 978	48 260	60 383	74 630	91 283	110 624	132 937	158 505	-
50	-	45 142	56 652	70 178	86 005	104 414	125 688	150 110	-
55	-	41 919	52 772	65 535	80 492	97 924	118 115	141 348	-
60	-	-	48 769	60 725	74 767	91 180	110 244	132 244	-
65	-	-	-	-	68 857	84 205	102 100	122 822	-

Power input in W

30	18 661	19 105	19 566	20 041	20 523	21 008	21 492	21 969	-
35	20 696	21 161	21 651	22 159	22 681	23 213	23 749	24 285	-
40	22 948	23 426	23 934	24 468	25 021	25 590	26 170	26 755	-
45	25 471	25 953	26 471	27 020	27 596	28 193	28 807	29 433	-
50	-	28 794	29 313	29 870	30 459	31 075	31 715	32 373	-
55	-	32 005	32 516	33 070	33 663	34 291	34 947	35 627	-
60	-	-	36 131	36 675	37 263	37 892	38 556	39 250	-
65	-	-	-	-	41 312	41 933	42 596	43 295	-

Current consumption in A

30	28.66	29.14	29.63	30.12	30.64	31.18	31.76	32.39	-
35	31.06	31.61	32.16	32.71	33.27	33.86	34.47	35.13	-
40	33.65	34.27	34.88	35.49	36.10	36.73	37.38	38.07	-
45	36.53	37.21	37.88	38.54	39.21	39.88	40.57	41.29	-
50	-	40.53	41.26	41.97	42.68	43.40	44.13	44.88	-
55	-	44.30	45.09	45.86	46.62	47.38	48.15	48.93	-
60	-	-	49.48	50.30	51.11	51.91	52.72	53.53	-
65	-	-	-	-	56.24	57.08	57.93	58.77	-

Mass flow in kg/h

30	883	1 092	1 335	1 616	1 940	2 311	2 733	3 211	-
35	875	1 085	1 329	1 611	1 935	2 306	2 729	3 207	-
40	864	1 075	1 319	1 601	1 925	2 296	2 718	3 196	-
45	851	1 062	1 306	1 587	1 911	2 281	2 702	3 179	-
50	-	1 046	1 289	1 570	1 892	2 261	2 680	3 155	-
55	-	1 028	1 269	1 548	1 869	2 235	2 653	3 125	-
60	-	-	1 246	1 523	1 841	2 205	2 620	3 089	-
65	-	-	-	-	1 809	2 170	2 581	3 048	-

Coefficient of performance (C.O.P.)

30	2.42	2.97	3.60	4.32	5.14	6.06	7.10	8.25	-
35	2.07	2.56	3.11	3.74	4.45	5.26	6.16	7.17	-
40	1.77	2.19	2.67	3.22	3.85	4.55	5.34	6.22	-
45	1.49	1.86	2.28	2.76	3.31	3.92	4.61	5.39	-
50	-	1.57	1.93	2.35	2.82	3.36	3.96	4.64	-
55	-	1.31	1.62	1.98	2.39	2.86	3.38	3.97	-
60	-	-	1.35	1.66	2.01	2.41	2.86	3.37	-
65	-	-	-	-	1.67	2.01	2.40	2.84	-

Nominal performance at to = 7.2 °C, tc = 54.4 °C

Cooling capacity	107 301	W
Power input	34 170	W
Current consumption	47.21	A
Mass flow	2 416	kg/h
C.O.P.	3.14	

Pressure switch settings

Maximum HP switch setting	29.5	bar(g)
Minimum LP switch setting	0.5	bar(g)
LP pump down setting	1	bar(g)

Sound power data

Sound power level		dB(A)
With accoustic hood		dB(A)

to: Evaporating temperature at dew point
tc: Condensing temperature at dew point
Rating conditions : Superheat = 11.1 K , Subcooling = 8.3 K

Tolerance according EN12900

FRCC.ED.SY380-4.B7.02 / page performance R407C 60 Hz

Heating and Cooling Coil Specifications

B

In fig. B.1 and B.3 on the next page the calculations for the cooling and heating coil operating in "Cooling Mode" can be seen.

Kapacitet	**136,71**	kW

Data luftside

Barometrisk tryk	**101,325**	kPa
Densitet	**1,225**	kg/m³
Luftmængde	**5,556**	m³/s
Lufthastighed	**1,58**	m/s
Tilgangstemperatur/RH	**27,00 / 60,0**	°C / %
Afgangstemperatur/RH	**15,00 / 97,4**	°C / %
S.H.R.	**0,62**	
Kondensat	**1,246**	l/min
Lufttryktab	**124**	Pa

Væskedata

Medium	**Ethylene Glycol 30%**	
Tilgang	**13,00**	°C
Afgang	**23,00**	°C
Væskemængde	**3,59**	l/s
Væskehastighed	**0,82**	m/s
Densitet	**1.046,128**	kg/m³
Væskevarmefylde	**3.638,00**	J/kg/K
Væske varmetrans	**0,450**	W/m/K
Viskositet	**2,388**	mPa.s
Tryktab	**55,3**	kPa

Fysiske data

Tør vægt	**512,3**	kg	Volume	**188,38**	dm³
Rør	**Cu: 0,35 x 12 mm**		Overfladeareal	**1.115,96**	m²
Stokke (L)	**Steel / Cu**		Lameller	**AL: 0,12 mm**	
Dim. [B" x H' x L']	**2.390 x 1.660 x 510**		Ramme	**Galv, 2,0mm**	
			Tilslutningsdim.	**1 x 2"**	Gevind

Figure B.1. Cooling Coil calculations by TT-Coil for "Cooling Mode".

Kapacitet	**20,93**	kW

Data luftside

Barometrisk tryk	**101,325**	kPa
Densitet	**1,225**	kg/m³
Luftmængde	**5,556**	m³/s
Lufthastighed	**1,58**	m/s
Tilgangstemperatur/RH	**15,00 / 97,4**	°C / %
Afgangstemperatur/RH	**18,00 / 80,3**	°C / %
Lufttryktab	**16**	Pa

Væskedata

Medium	**Ethylene Glycol 30%**	
Tilgang	**23,00**	°C
Afgang	**21,47**	°C
Væskemængde	**3,59**	l/s
Væskehastighed	**1,36**	m/s
Densitet	**1.044,358**	kg/m³
Væskevarmefylde	**3.651,48**	J/kg/K
Væske varmetrans	**0,455**	W/m/K
Viskositet	**2,086**	mPa.s
Tryktab	**33,2**	kPa

Fysiske data

Tør vægt	**87,7**	kg	Volume	**31,33**	dm³
Rør	**Cu: 0,35 x 12 mm**		Overfladeareal	**125,42**	m²
Stokke (L)	**Steel / Cu**		Lameller	**AL: 0,12 mm**	
Dim. [B" x H' x L']	**2.390 x 1.660 x 130**		Ramme	**Galv, 2,0mm**	
			Tilslutningsdim.	**1 x 2"**	Gevind

Figure B.2. Heating Coil calculations by TT-Coil for "Cooling Mode".

In fig. B.3 the calculations for the heating coil operating in "Heating Mode" can be seen.

Kapacitet	**89,30**	kW

Data luftside

Barometrisk tryk	**101,325**	kPa
Densitet	**1,225**	kg/m³
Luftmængde	**5,556**	m³/s
Lufthastighed	**1,58**	m/s
Tilgangstemperatur/RH	**17,00 / 15,0**	°C / %
Afgangstemperatur/RH	**30,00 / 6,3**	°C / %
Lufttryktab	**111**	Pa

Væskedata

Medium	**Ethylene Glycol 30%**	
Tilgang	**32,00**	°C
Afgang	**25,50**	°C
Væskemængde	**3,59**	l/s
Væskehastighed	**0,82**	m/s
Densitet	**1.041,560**	kg/m³
Væskevarmefylde	**3.671,82**	J/kg/K
Væske varmetrans	**0,463**	W/m/K
Viskositet	**1,728**	mPa.s
Tryktab	**51,8**	kPa

Fysiske data

Tør vægt	**512,3**	kg	Volume	**188,38**	dm³
Rør	**Cu: 0,35 x 12 mm**		Overfladeareal	**1.115,96**	m²
Stokke (L)	**Steel / Cu**		Lameller	**AL: 0,12 mm**	
Dim. [B" x H' x L']	**2.390 x 1.660 x 510**		Ramme	**Galv, 2,0mm**	
			Tilslutningsdim.	**1 x 2"**	Gevind

Figure B.3. Heating Coil calculations by TT-Coil for "Heating Mode".

The coil consists of two sections, as seen for "Cooling Mode" the section cools down and condenses moist content of the air. This process heats up the EG/water mixture which is the sent through the other sections of the coil. In the second section the air reheated around 3 K utilizing the energy absorbed from the air in the first sections. As for "Heating Mode" the two coils are both used for heating and in the calculations they are considered as one unit.

Cooling Tower Performance C

The in fig. C.1 the performance and power consumption for a Vestas Aircoil cooling tower can be seen. The data has been provided by Danfoss and will be used to determine the inlet temperature of the cooling water in the model of the heat pump system.

Wet Bulb	Temp. Dr	RH	Inlet	Outlet	Hour/year	Flow	Cooling	Power kW	HZ	RPM	Power	
Twb	Tempe rature	Rel. Humidit y	Twi	Two	Hour	m3/h	Heat kW	Samlet motore ffekt	Frekve ns	Omdrej ningsta l	Motoref fekt	Forda mpning
0	0	100%	21	16	1759	100	581	0	0			0,7
1	1,4	93%	21	16	2207	100	581	0	0			0,7
2	2,8	88%	21	16	2647	100	581	0	0			0,7
3	4,2	82%	21	16	3132	100	581	0	0			0,7
4	5,6	78%	21	16	3593	100	581	0	0			0,7
5	7	74%	21	16	4024	100	581	0	0			0,7
6	8,4	71%	21	16	4430	100	581	0	0			0,7
7	9,8	68%	21	16	4841	100	581	0	0			0,7
8	11,2	65%	21	16	5235	100	581	0	0			0,7
9	12,6	53%	21	16	5641	100	581	0	0			0,7
10	14	61%	21	16	6081	100	581	0	0			0,7
11	15,4	59%	21	16	6616	100	581	0	0			0,7
12	16,8	57%	21	16	7100	100	581	13,18	50	580	13,18	0,7
13	18,2	56%	21,6	16,6	7476	100	581	13,14	50	580	13,14	0,7
14	19,6	54%	22,4	17,4	7883	100	581	13,08	50	580	13,08	0,7
15	21	53%	23,2	18,2	8203	100	581	13,02	50	580	13,02	0,7
16	22,4	52%	24	19	8476	100	581	12,96	50	580	12,96	0,7
17	23,2	51%	24,8	19,8	8611	100	581	12,9	50	580	12,9	0,7
18	25,2	50%	25,7	20,7	8690	100	581	12,84	50	580	12,84	0,7
19	26,6	49%	26,5	21,5	8734	100	581	12,79	50	580	12,79	0,7
20	28	49%	27,3	22,3	8752	100	581	12,73	50	580	12,73	0,7
21	29,4	48%	28,2	23,2	8759	100	581	12,67	50	580	12,67	0,7
22	30,8	47%	29	24	8760	100	581	12,61	50	580	12,61	0,7
23	32,2	47%	29,9	24,9	-	100	581	12,55	50	580	12,55	0,7
24	33,6	46%	30,7	25,7	-	100	581	12,5	50	580	12,5	0,7
25	35	46%	31,6	26,6	-	100	581	12,46	50	580	12,46	0,7

Figure C.1. Cooling tower data for an Vestas Aircoil cooling tower.